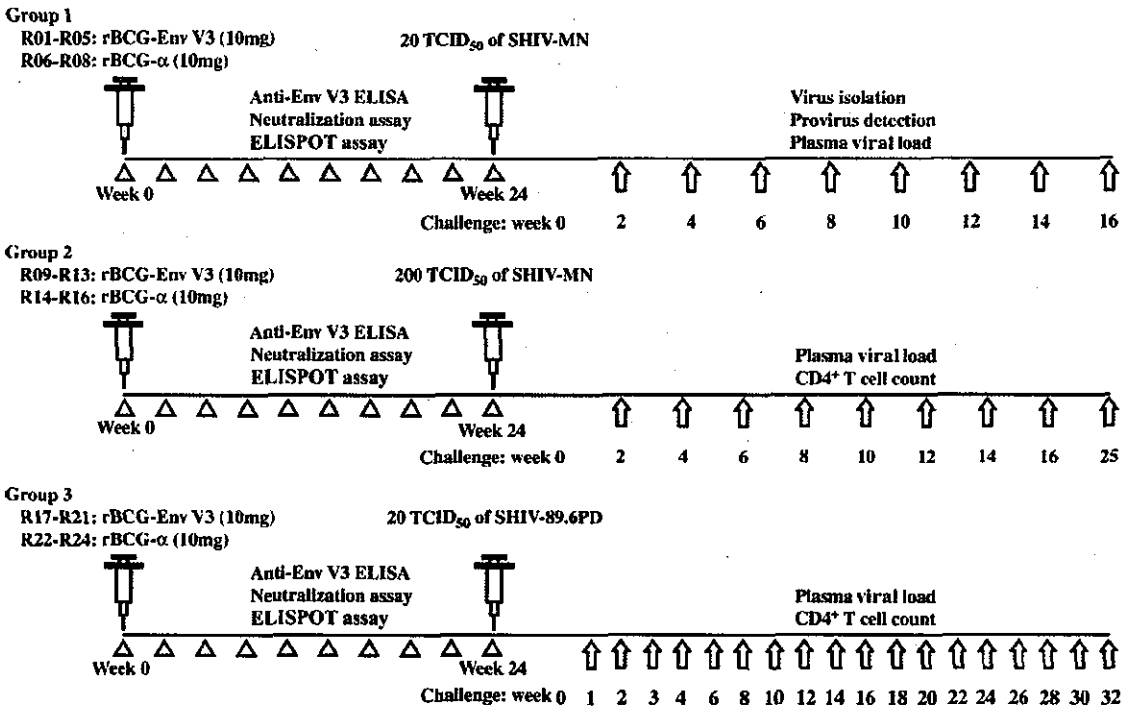

FIG. 1. Schematic representation of the experimental protocol for immunization of rhesus macaques with rBCG Env V3 and challenge with either SHIV-MN or SHIV-89.6PD. A total of 24 macaques were assigned to either the rBCG Env V3 vaccine or rBCG vector control group. The animals each received a single subcutaneous injection and were then split into three groups prior to challenge with either low-dose SHIV-MN, high-dose SHIV-MN, or SHIV-98.6PD.

rBCG Env V3 (16), which expresses and secretes a chimeric protein consisting of α-antigen and the Env V3 region of HIV-1_{MN}. The remaining nine macaques were immunized by the same route and with the same dose of rBCG α-antigen and served as vector controls. All macaques inoculated with rBCG Env V3 remained in good health following vaccination. Three of the 15 immunized macaques experienced transient redness with slight erosion localized at the injection site; however, the reaction spontaneously resolved within 3 months. Following immunization, the 24 macaques were divided into three groups, each group consisting of five immunized animals and three vector controls. The macaques within each group received an intravenous challenge with either SHIV-MN (20 or 200 $TCID_{50}$) or SHIV-89.6PD (20 $TCID_{50}$) (Fig. 1).

Vaccine-induced HIV-specific immune responses following rBCG Env V3 immunization. (i) Neutralizing antibodies. As described above, 15 rhesus macaques were vaccinated with a single subcutaneous inoculation of 10 mg of rBCG Env V3. Induction of HIV-1-specific immunity was measured 24 weeks later in blood samples obtained pre- and postvaccination. All 15 immunized macaques exhibited HIV-1 Env V3 peptide-binding antibody activity by ELISA at serum dilutions ranging from 1:640 to 1:10,240 (Fig. 2). Antibody responses were monophasic, peaking at 4 to 6 weeks and then gradually declining. Serum samples obtained from naïve macaques were consistently negative by ELISA, while postvaccination sera did not react with a control fusion peptide of HIV gp41 (data not shown).

Antibodies were purified from the macaque sera to remove factors that might interfere with certain bioassays (51). The purified antibodies were then tested in vitro for the ability to neutralize SHIV-MN infection in M1866 cells (Fig. 3). Antibodies induced in macaques vaccinated with rBCG Env V3 strongly neutralized both the challenge SHIV-MN (grown in rhesus PBMC) and a T-cell line-adapted (TCLA) laboratory strain, HIV-1_{MN}. A mean 50% inhibitory concentration (IC_{50}) of 0.05 to 0.5 μg of IgG/ml was measured against SHIV-MN, and a mean IC_{90} of ~3.0 μg of IgG/ml was observed against HIV-1_{MN}. Neutralizing activity was detected in serum samples obtained 4 to 6 weeks after vaccination and was maintained for at least 24 weeks. Preimmune serum IgG from nine macaques immunized with vector alone, and IgG from three additional naive macaques (data not shown), did not neutralize either virus.

(ii) Neutralization responses against primary HIV-1 isolates. To further assess the specificity of antibodies in immune sera, neutralizing activity was evaluated against a panel of seven primary HIV-1 isolates using GHOST cells expressing either CCR5 or CXCR4 (Table 1). Purified IgG from macaques in each of the three immunization groups was able to effectively neutralize HIV-$1_{BZ167/X4}$, HIV-$1_{SF2/X4}$, and HIV-$1_{CI2/X4}$ (Table 1 and Fig. 4), with mean IC_{50} values of 5 to 7, 4 to 7, and 5 to 15 μg/ml, respectively. By comparison, neutralization of HIV-$1_{MNp/X4}$ required ~10-fold more serum IgG, with a mean IC_{50} of 50 μg/ml. Three additional isolates, HIV-$1_{SF33/X4}$, HIV-$1_{SF33/R5}$, and the clade A isolate HIV-$1_{VI313/R5}$,

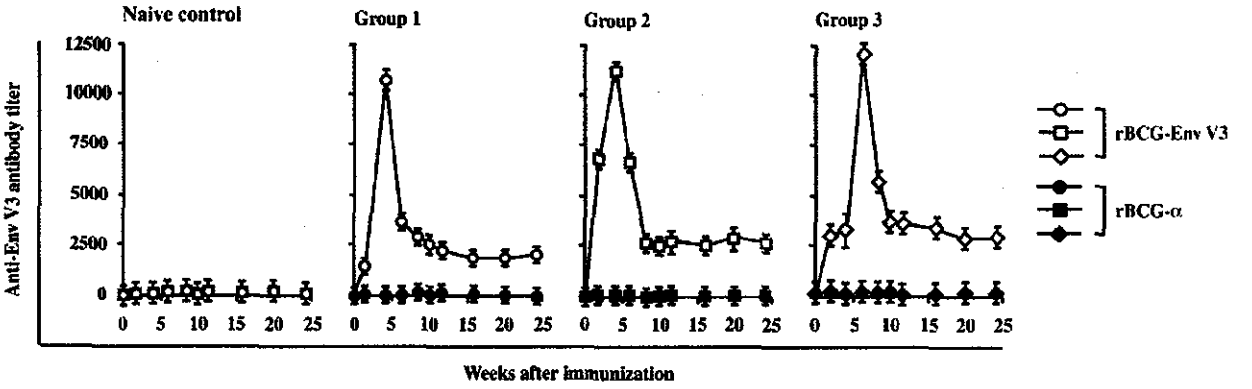

FIG. 2. Serum anti-V3 antibody titers determined by peptide-based ELISA. Preimmune and immune sera from macaques inoculated with rBCG Env V3 were collected and stored at −80°C until they were used. Sera from naïve macaques were used as controls. Data using preimmune sera were within the control levels (data not shown). The results are expressed as the means ± SD of four independent assays.

were not neutralized with serum IgG concentrations up to 50 μg/ml (Table 1). Preimmune sera had no neutralizing activity against any of the isolates. Thus, antibodies present in sera from the immunized macaques were able to neutralize primary HIV-1 isolates, including HIV-1_{BZ167}, HIV-1_{SF2}, and HIV-1_{CI2}, in assays using GHOST cells that express CXCR4 with 10- to 50-fold-higher sensitivity than that of the dual-tropic (X4-R5) TCLA strain HIV-1_{MNp}. Among the neutralization-sensitive viruses, the V3 sequence motifs of HIV-1_{BZ167} and HIV-1_{SF2} shown in Fig. 5 did not correlate with the observed neutralization profiles of HIV-1 Env V3.

(iii) V3 peptide-specific T-cell responses. Table 2 offers a comparison of the virus-specific T-cell response levels determined by IFN-γ ELISPOT analysis in immunized animals with the neutralization data provided in Fig. 2. Of the 15 animals immunized with rBCG Env V3 (180 and 160 SFC/10^6 PBMC at 6 weeks postimmunization [p.i.], respectively), only R-09 and R-10 showed very low levels of SFC activities at the time of

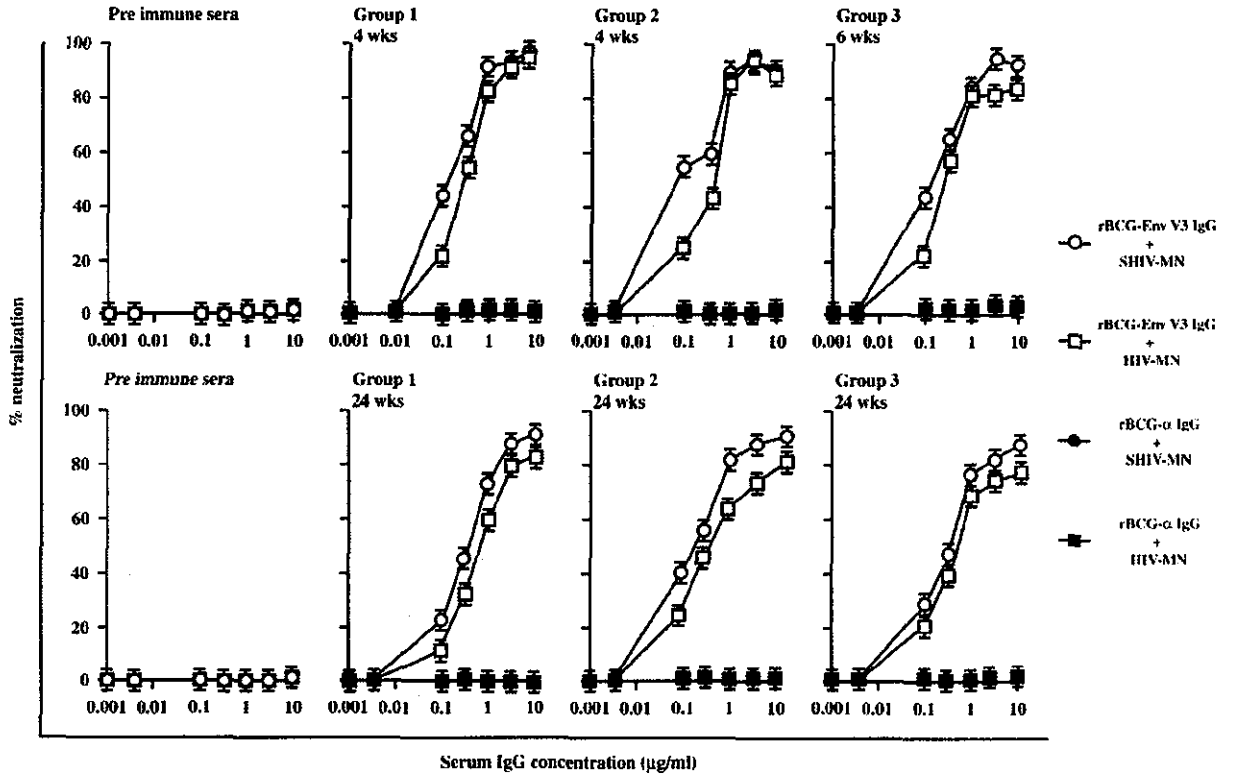

FIG. 3. HIV-1-specific neutralization antibody responses in macaques vaccinated with rBCG Env V3. Analysis of in vitro neutralization of SHIV-MN by anti-rBCG-HIV-1 antibodies using M8166 cell-based virus neutralization assays. Serum IgG was purified from preimmune or immune sera of macaques inoculated with rBCG Env V3 at the indicated times. The results are expressed as the means ± SD of four independent assays.

TABLE 1. 50% neutralization calculated on the basis of neutralization curves[a]

Serum sample	Neutralizing activity (μg)						
	BZ167/X4	MNp/X4	SF2/X4	SF33/X4	SF33/R5	V1313/R5	C12/X4
Group 1	6.5	50	7	>50	>50	>50	10
Group 2	5	50	4	>50	>50	>50	5
Group 3	7	50	6.5	>50	>50	>50	15
Pre immunization sera of groups 1, 2, and 3	>50	>50	>50	>50	>50	>50	>50

[a] The neutralization assays with the various viruses were carried out in GHOST cells expressing either CXCR4 (X4) or CCR5 (R5) as indicated in Fig. 4. BZ167, MNp, SF2, SF33, and CI-2 are HIV-1 clade B viruses. V1313 is an HIV-1 clade A virus.

SHIV challenge (120 and 110 SFC/10^6 PBMC at 24 weeks p.i., respectively) (Table 2). In contrast, <100 SFC/10^6 PBMC were observed in other immunized animals, and <20 SFC/10^6 PBMC were observed in controls. Thus, the V3 region antigen in the rBCG Env V3 proved unable to induce significant levels of virus-specific T-cell responses in immunized animals.

Challenge with low-dose SHIV-MN. The first group of eight macaques (R-01 through R-08), consisting of five animals that received rBCG Env V3 and three that received control rBCG α-antigen, were intravenously challenged with low-dose SHIV-MN (20 $TCID_{50}$) at 24 weeks p.i. The cell-associated virus load was measured in PBMC cocultures, and proviral copy numbers were estimated by DNA PCR using primary PBMC genomic DNA. The level of plasma viremia in each macaque was quantified by competitive reverse transcription-PCR to assess infection and virus replication for 16 weeks after virus challenge (Table 3).

Control macaques vaccinated with the vector alone (R-06 through R-08) were positive in all three viral-load assays 2 weeks after SHIV-MN challenge and remained positive for a follow-up period of 10 weeks. Because only low levels of viral RNA (<10^4 RNA copies/ml) were transiently detected 2 weeks postchallenge, all three assays (virus isolation, plasma RNA, and proviral DNA) were used for virus detection. Using these criteria, we observed that all three parameters remained negative after low-dose SHIV-MN challenge in three of five macaques vaccinated with rBCG Env V3 (R-02, R-04, and R-05). However, macaque R-01 was transiently positive in all three assays for virus infection at 4 weeks. Another macaque immunized with rBCG Env V3 (R-03) exhibited a sharp in-

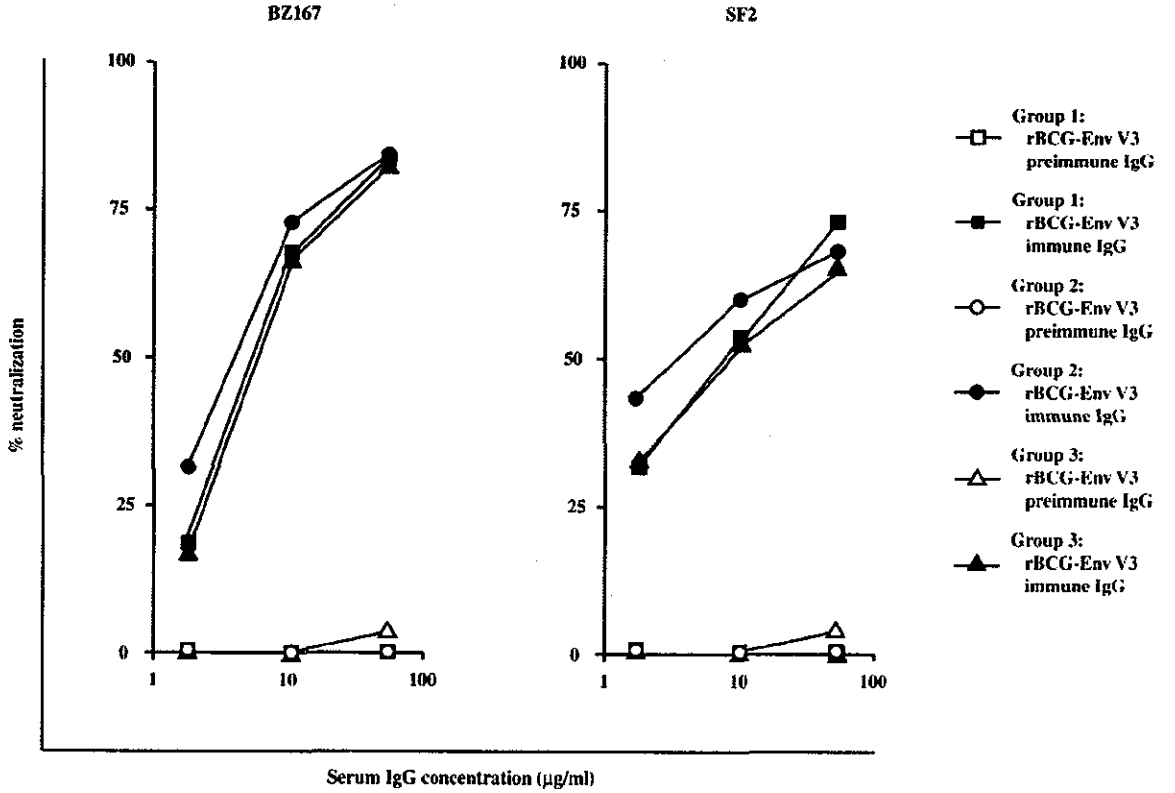

FIG. 4. Neutralization of HIV-1_{BZ167} and HIV-1_{SF2} in GHOST-X4 cells by immune sera from macaques vaccinated with rBCG Env V3. Dilutions of immune sera (closed symbols) and preimmune sera (open symbols) were tested in duplicate, and the percent neutralization was calculated using the mean value. The dose-response curves represent the means of three independent assays.

```
MN      CTRPNYNKRKRIHI  GPGRAFYTTKNIIGTIRQAHC
BZ167   -----NKA-R--R-  ----T---G- -V-D----Y-
SF2     ---LSN-T--C-PL  ----V--A-DI- -D------
CI2     ----SN-T-R----  ---------RQ-R-D------
MNp     -----N-R-T----  --------------------

89.6P   -----N-T-E-LS-  --------ARR----D------
SF33    -----N-R-R--TS  ---KVL---GE---D--K-Y-
VI131   -----N-T-QSV--  ---Q---A-GDV--D------
IIIB    -----N-T---KS-QR------V-IGK- -NM-----
```

FIG. 5. Alignment of the amino acid sequences of HIV-1 Env V3 from primary and laboratory isolates. The spaces indicate amino acid deletions; dashes indicate homology. The V3 motif of a neutralization-sensitive HIV-1 strain is enclosed in the shaded rectangle (37).

crease in viral load following challenge, and the levels remained high until the animal was sacrificed. These results demonstrate that vaccination with rBCG Env V3 can induce protective immunity in rhesus macaques *against* a low-dose challenge with SHIV-MN.

Challenge with high-dose SHIV-MN. The second group of eight macaques (R-09 through R-16) was similarly challenged with a higher dose (200 $TCID_{50}$) of SHIV-MN by intravenous inoculation at 24 weeks p.i. (Fig. 6). Measurements of the viral loads in PBMC and plasma indicated that all the macaques were infected by the high-dose SHIV-MN challenge. However, the level of viremia during the acute phase of viral infection was reduced by 1 to 2 log units in macaques immunized with rBCG Env V3 compared with controls (from 10^6 to 10^7, to $<10^5$ to 10^4 RNA copies/ml) (Fig. 6A). The control macaques developed a transient decrease in $CD4^+$-T-cell counts that rebounded to normal levels ~3 weeks postchallenge (*Fig. 6B*). In contrast, macaques vaccinated with rBCG Env V3 had little or no change in $CD4^+$-T-cell numbers.

Despite the low levels of V3 peptide-specific IFN-γ ELISPOT activities noted for animals R-09 and R-10 above (Table 2), these animals exhibited a plasma viral load and a rate of $CD4^+$-cell loss after SHIV challenge that was comparable to those seen in the immunized animals designated R-11, -12, and -13. Thus, immunization with rBCG Env V3 generated even low levels of T-cell responses in only 2 animals out of 5 in this group and out of a total of 15 immunized animals. No evidence of higher virus-specific IFN-γ ELISPOT activity was demonstrated in samples obtained 0, 4, or 6 and 24 weeks after vaccination (Table 2), suggesting that few significant cellular anti-SHIV responses were generated and that those few did not affect virus control in this macaque population.

Challenge with pathogenic SHIV-89.6PD. The third group of macaques (R-17 through R-24) was challenged with pathogenic SHIV-89.6PD (20 $TCID_{50}$) 24 weeks postinoculation. The effects of vaccination with rBCG Env V3 on immune induction against the pathogenic virus were followed for 32 weeks, and the macaques were then autopsied. As shown in

TABLE 2. SHIV-MN-specific serum IgG neutralization titers and Env V3-specific ELISPOT responses[a]

Monkey no.	Immunogen	IC_{50} of neutralization serum IgG (μg/ml)[b]			V3-specific IFN-γ SFCs/10^6 cells[c]		
		0 week	4 or 6 weeks[d]	24 weeks[e]	0 week	4 or 6 weeks	24 weeks
R-01	rBCG Env V3	>50	0.5	0.6	<20	30	20
R-02	rBCG Env V3	>50	0.3	0.4	<20	40	40
R-03	rBCG Env V3	>50	0.5	0.6	<20	40	30
R-04	rBCG-Env V3	>50	0.2	0.3	<20	20	40
R-05	rBCG-Env V3	>50	0.08	0.3	<20	30	80
R-06	rBCG-α	>50	>50	>50	<20	<20	<20
R-07	rBCG-α	>50	>50	>50	<20	<20	<20
R-08	rBCG-α	>50	>50	>50	<20	<20	<20
R-09	rBCG-Env V3	>50	0.04	0.3	<20	180	120
R-10	rBCG-Env V3	>50	0.1	0.2	<20	160	110
R-11	rBCG-Env V3	>50	0.05	0.2	<20	20	30
R-12	rBCG-Env V3	>50	0.03	0.4	<20	60	20
R-13	rBCG-Env V3	>50	0.02	0.4	<20	30	30
R-14	rBCG-α	>50	>50	>50	<20	<20	<20
R-15	rBCG-α	>50	>50	>50	<20	<20	<20
R-16	rBCG-α	>50	>50	>50	<20	<20	<20
R-17	rBCG-Env V3	>50	0.2	0.6	<20	40	90
R-18	rBCG-Env V3	>50	0.3	0.3	<20	50	60
R-19	rBCG-Env V3	>50	0.3	0.4	<20	40	30
R-20	rBCG-Env V3	>50	0.5	0.7	<20	20	50
R-21	rBCG-Env V3	>50	0.4	0.5	<20	20	40
R-22	rBCG-α	>50	>50	>50	<20	<20	<20
R-23	rBCG-α	>50	>50	>50	<20	<20	<20
R-24	rBCG-α	>50	>50	>50	<20	<20	<20

[a] Animals were inoculated with either rBCG Env V3 or the vector control. Blood samples were obtained at 0, 4, or 6 and 24 weeks p.i., and antibody inhibitory concentration and the V3-specific IFN-γ ELISPOT activity were compared.
[b] The IC_{50} was derived from the data in Fig. 2 based on neutralization dose-response curves similarly obtained from Fig. 3.
[c] Freshly isolated PBMC were assessed for their ability to produce IFN-γ in response to $HIV\text{-}1_{MN}$ Env V3 peptide.
[d] Mean IC_{50}s: R-01 to R-05, 0.32; R-09 to R-13, 0.05; R-17 to R-21, 0.35.
[e] Mean IC_{50}s: R-01 to R-05, 0.44; R-09 to R-13, 0.30; R-17 to R-21, 0.50.

TABLE 3. Comparison of low-dose SHIV-MN infections in macaques vaccinated with either rBCG Env V3 or rBCG-α (control)

Monkey	Immunogen (10 mg)	Efficacy analysis	Results[a]							
			0[b]	2	4	6	8	10	12	16
R-01	rBCG Env V3	Virus isolation	<1	<1	2	<1	<1	<1	<1	<1
		Provirus by PCR	<500	<500	>500	<500	<500	<500	<500	<500
		Plasma viral load	<500	<500	20,000	<500	<500	<500	<500	<500
R-02	rBCG Env V3	Virus isolation	<1	<1	<1	<1	<1	<1	<1	<1
		Provirus by PCR	<500	<500	<500	<500	<500	<500	<500	<500
		Plasma viral load	<500	<500	<500	<500	<500	<500	<500	<500
R-03	rBCG Env V3	Virus isolation	<1	32	<1	<1	2	<1	ND	ND
		Provirus by PCR	<500	>500	<500	<500	>500	<500	ND	ND
		Plasma viral load	<500	310,000	<500	<500	20,000	<500	ND	<500
R-04	rBCG Env V3	Virus isolation	<1	<1	<1	<1	<1	<1	ND	ND
		Provirus by PCR	<500	<500	<500	<500	<500	<500	ND	ND
		Plasma viral load	<500	<500	<500	<500	<500	<500	<500	<500
R-05	rBCG Env V3	Virus isolation	<1	<1	<1	<1	<1	<1	<1	ND
		Provirus by PCR	<500	<500	<500	<500	<500	<500	<500	ND
		Plasma viral load	<500	<500	<500	<500	<500	<500	<500	<500
R-06	rBCG-α	Virus isolation	<1	32	16	<1	2	2	<1	1<
		Provirus by PCR	<500	>500	>500	>500	>500	>500	>500	500
		Plasma viral load	<500	300,000	50,000	20,000	20,000	20,000	20,000	20,000
R-07	rBCG-α	Virus isolation	<1	2	32	<1	<1	<1	<1	ND
		Provirus by PCR	<500	>500	>500	>500	>500	<500	<500	ND
		Plasma viral load	<500	27,000	310,000	350,000	25,000	<500	<500	<500
R-08	rBCG-α	Virus isolation	<1	32	16	<1	2	2	ND	ND
		Provirus by PCR	<500	>500	>500	>500	>500	>500	ND	ND
		Plasma viral load	<500	300,000	50,000	<500	20,000	20,000	ND	<500

[a] Viral loads were determined by either limiting dilution of PBMC or competitive PCR for HIV-1 Env V3 genes, and the results are expressed as the number of infected cells per million PBMC and virus copies per milliliter of blood. Nested PCR for HIV-MN Env V3 was used in all macaques to detect the provirus genome. Naïve macaques were injected intravenously with 20 $TCID_{50}$ of SHIV-MN and used as controls for SHIV infection. The results are expressed as the mean of three different assays; <1, <500, and <500 were the detection limits of virus isolation, proviral copy number, and plasma viral load, respectively. ND, not determined.
[b] Weeks after challenge.

Fig. 7, high levels of plasma viremia were detected in the control macaques, with a viral set point of ~10^6 RNA copies/ml, accompanied by an abrupt decline in $CD4^+$-T-cell counts. Prior vaccination with rBCG Env V3 appeared to have no positive effect on the viral load and $CD4^+$-T-cell counts compared with the control animals.

Association of in vitro neutralization antibody responses following rBCG Env V3 immunization with control of viremia after SHIV challenge. Of the macaques challenged with low doses of homologous SHIV-MN (group 1), the three virus-controlled macaques R-02, -04, and -05 (Table 1) had higher IC_{50}s of SHIV-MN-specific neutralizing antibodies as measured in M8166 cells at 24 weeks p.i. or on the day of challenge, with serum IgG concentrations of 0.4, 0.3, and 0.3 μg/ml, respectively (Table 2). The IC_{50}s of the uncontrolled macaques R-01 and -03 (Table 1) were both 0.6 μg/ml (Table 2).

When the challenge dose was increased 10-fold (Fig. 1), all five animals in group 2 had high neutralizing antibody titers with a mean IC_{50} of 0.30 μg/ml on the day of challenge (Table 2). These animals in group 2 showed partial protection against the same homologous virus challenge (Fig. 6). In contrast, no animals similarly immunized with rBCG elicited any in vivo protection against a low-dose, heterologous viral challenge with SHIV-89.6PD (Table 2 and Fig. 7).

In summary, the rBCG Env V3-elicited NAb response afforded some degree of protection against a homologous viral challenge. However, infection by the heterologous virus SHIV-89.6PD was not controlled by heterologous virus SHIV-MN- or $HIV\text{-}1_{MN}$-specific NAb generated by the recombinant $HIV\text{-}1_{MN}$ Env V3-expressed BCG immunization.

DISCUSSION

First, our study demonstrates the potential of anti-Env V3 NAb induced by immunization of rhesus macaques with rBCG Env V3 to afford protection against homologous challenge with SHIV-MN but not against the heterologous SHIV-89.6PD. With the low-dose homologous SHIV-MN challenge (20 $TCID_{50}$), sterile protection was achieved in three of five immunized animals. These findings correlate well with our in vitro neutralization data for these animals. Protected animals showed higher levels of potent neutralization antibodies than did unprotected animals. Macaques serving as vector and naïve controls experienced high levels of replication of the SHIV-MN challenge virus. With a high-dose challenge, rBCG Env V3 vaccination was effective at reducing viremia during acute infection by ~100-fold. The vaccine consisted of an rBCG vector that expresses a chimeric HIV-1 Env V3 region peptide and the α-antigen of *M. bovis*. The kinetics and magnitude of the HIV-1 Env V3-specific antibody responses elicited in macaques were comparable to those observed in our previous studies using guinea pigs vaccinated with rBCG Env V3 (9, 16).

Secondly, the levels of neutralizing antibodies generated after injection with a recombinant BCG vector-based vaccine expressing a chimeric protein of HIV-1 Env V3 peptide and α-antigen protein were maintained for at least 24 weeks p.i. with no diminishment in titer. A plausible explanation for the longevity of the neutralizing antibody titers after rBCG immunization is that the carrier protein, α-antigen (also known as MPT59 or antigen 85B), is derived from mycobacteria and has

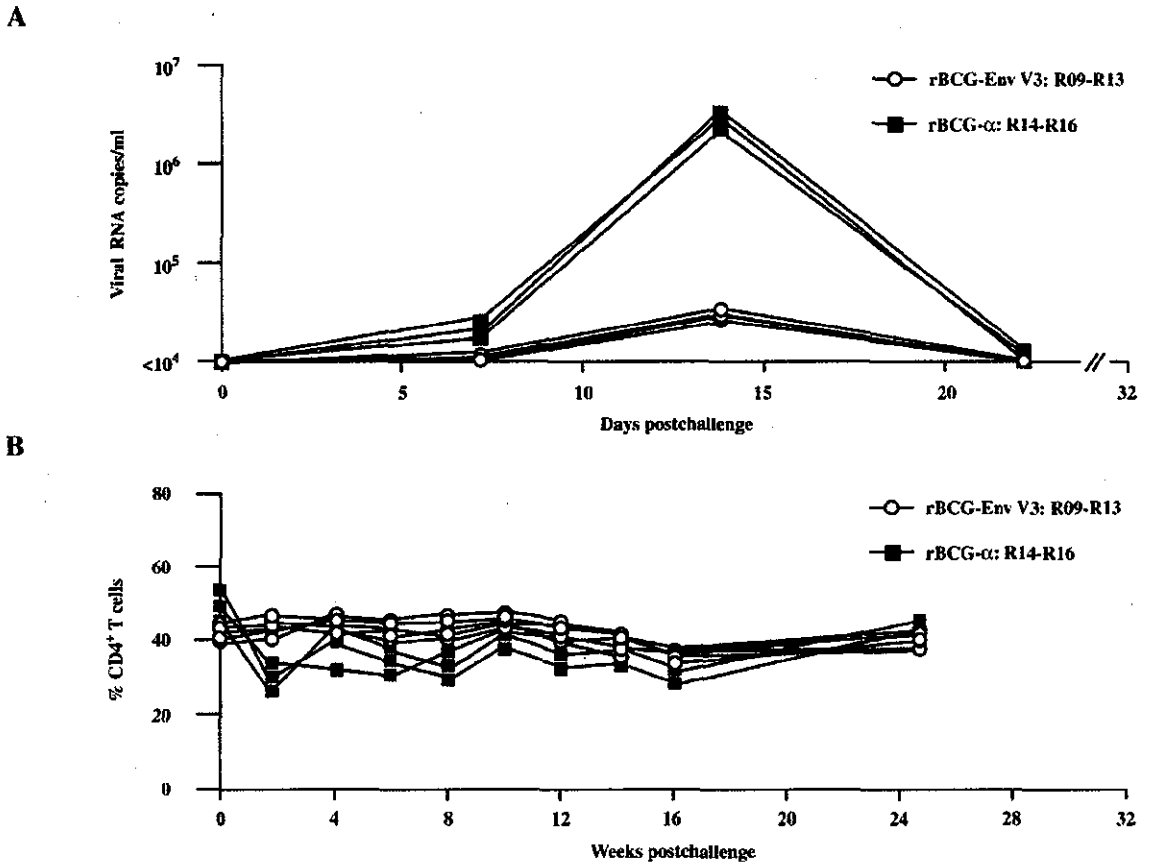

FIG. 6. Comparison of infection kinetics following high-dose (200 $TCID_{50}$) inoculation of SHIV-MN in macaques vaccinated with either rBCG Env V3 or rBCG vector control. (A) Viral RNA copy number per milliliter of serum. (B) $CD4^+$-T-cell count as a percentage of total lymphocytes. The results in individual animals are expressed.

the ability to elicit potent Th1-type immune responses (24, 43). Our result is consistent with those of other groups, which have shown that BCG immunity is maintained for at least a few years and that the BCG bacillus is effective at increasing NAb responses (40). These characteristics might help to explain the long-lasting enhanced levels of NAb elicited by vaccination with rBCG Env V3.

The concentration of purified macaque IgG in serum was determined to be ~10 mg/ml. By this estimation, 0.5 mg corresponds to a serum dilution of 1:1 in virus neutralization assays. The IC_{50} and IC_{90} values for neutralization of SHIV-MN were 10^3 to 10^4 and 166, respectively (similar values were obtained for neutralization of HIV-1_{MN}). These neutralization titers suggest that antibody responses generated de novo may contribute to a degree of protection against SHIV-MN. The observed relationship of the NAb titer and viral protection is consistent with results obtained by repeated immunization with SHIV-89.6 C4-V3 peptides in guinea pigs and rhesus macaques (6, 27). In this case, NAb titers to homologous SHIV-89.6 were ~10^3 greater than those against heterologous HIV-1_{MN}, while responses to HIV-1 R5 viruses were weak or absent. This suggests that the protection mediated by a C4-V3 peptide vaccine against SHIV-89.6 may be type (or strain) specific. Thus, we assume that the NAb generated by SHIV-89.6 C4-V3 peptide immunization (6) would not mediate protection against a heterologous SHIV-MN challenge.

The present study suggests that the vaccine-elicited antibodies directed against the HIV-1 Env V3 peptide can in some cases confer a degree of neutralization against primary isolates of HIV-1 (26). Following vaccination of rhesus macaques with rBCG Env V3, both binding and NAb responses against this novel construct were clearly evident. At the time of SHIV challenge, immune sera from the vaccinated macaques efficiently neutralized a homologous, type-specific TCLA HIV-1 strain (HIV-1_{MN}) and a related SHIV strain (SHIV-MN) with IC_{90} values of <5 μg/ml. Controls, including preimmune sera and sera from macaques vaccinated with rBCG vector alone, had no neutralizing activity in assays using GHOST cells expressing either CCR5 or CXCR4 or in M8166 cells. Immune sera from macaques vaccinated with rBCG Env V3 were able to neutralize several primary HIV-1 X4 isolates (HIV-1_{BZ167}, HIV-1_{SF2}, and HIV-1_{CI2}); however, neutralization of an X4-R5 dual-tropic strain (HIV-1_{MNp}) was weak. No neutralization of HIV-1 R5 isolates and primary HIV-1 isolates from different clades was observed. These findings were confirmed in an independent international neutralization trial (conducted by Simon Beddows and Jonathan Weber, Imperial College School of Medicine, Medical Research Council, London, En-

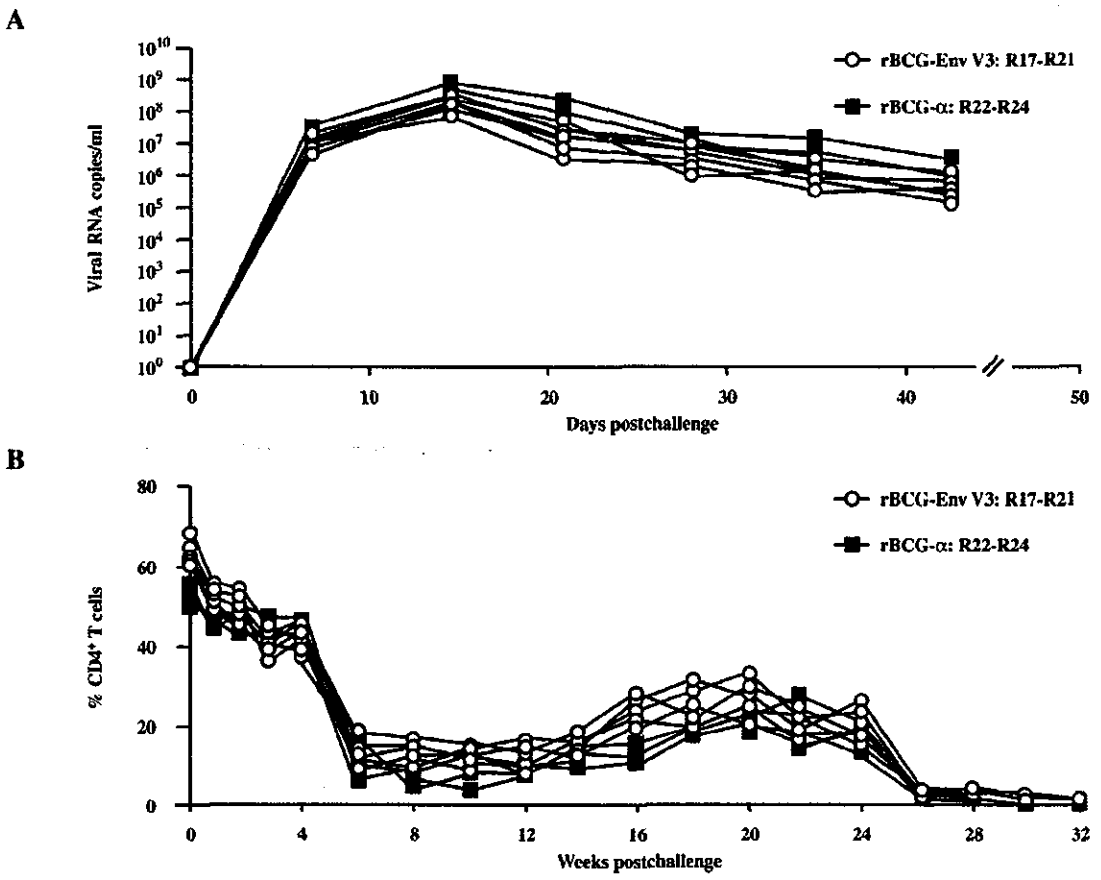

FIG. 7. Comparison of infection kinetics following challenge with pathogenic SHIV-89.6PD in macaques vaccinated with either rBCG Env V3 or rBCG vector control. (A) Plasma viral-RNA copy numbers per milliliter. (B) $CD4^+$-T-cell count as a percentage of total lymphocytes. The results in individual animals are expressed.

gland, and Pia Scott and Eva-Maria Fenyo at Microbiology and Tumorbiology Center, Karolinska Institute, Stockholm, Sweden). Preliminary results from this study have had been summarized and reported (11). Despite similarities in the V3 sequence motif, neutralization of the TCLA strain HIV-1_{MN} was found to be 10- to 50-fold more sensitive than neutralization of primary HIV-1 isolates, such as HIV-1_{CI2}, HIV-1_{MNp}, or HIV-$1_{JR\text{-}CSF}$ (11). A reasonable explanation for the relative insensitivity of primary HIV-1 isolates—particularly primary HIV-1 R5 isolates—to neutralization is the presence of cryptic or occluded sites within the virus-associated V3 region (13, 53).

In the Japanese consensus HIV-1 Env V3 expressed in the rBCG construct, the core V3 motif of the neutralization epitope is IHIGPGRAF (39). Although the consensus sequence of the V3 loop differs from the MN-V3 sequence in five amino acid positions, the neutralization epitope of the tip V3 region in the Japanese consensus is identical to that of MN-V3. Some substitutions of amino acids at certain positions within this motif (for example, H to R and A to T in the core motif in BZ167) are tolerated, suggesting that NAbs generated by immunization with rBCG Env V3 are not strictly type specific. Immune sera from macaques vaccinated with rBCG Env V3 were able to neutralize primary HIV-1 X4 and some HIV-1 X4-R5 dual-tropic isolates, suggesting that the antigenic structure of the chimeric V3 peptide mimics to some extent that of the virus-associated V3 region. Indeed, the chimeric V3–α-antigen protein is estimated to be 38 kDa and contains four cysteine residues, suggesting the possible formation of a new loop structure in the V3 portion of the protein. With regard to the heterologous SHIV-89.6PD challenge in macaques vaccinated with rBCG Env V3, NAbs specific for SHIV-89.6PD were not generated efficiently (IC_{50}, >50 μg of immune serum IgG/ml) and did not provide any protection against the SHIV-89.6PD challenge. The V3 neutralization site of SHIV-89.6PD may differ in sequence or structure or both from that of SHIV-MN or other viral strains, including some of the HIV-1 isolates, making it unrecognizable to antibodies. Such a difference could account for the poor cross-neutralization activity against SHIV-89.6PD.

Thus, our data from the SHIV-macaque models show that the in vitro neutralization titers generated in rBCG-immunized animals correlate with protection. Although a present goal of HIV-1 vaccine development is to reduce the viral set point by eliciting high levels of virus-specific cellular immune responses, induction of cross-reactive NAbs may also contribute to control virus replication in the course of HIV-1 infection and may therefore be useful in the context of a preventive vaccine. Furthermore, although the choice of HIV Env V3 and the

autologous challenge virus SHIV-MN are unlikely to provide information that predicts efficacy in humans, the results presented here demonstrate that recombinant BCG vectors have the potential to deliver a more appropriate immunogen for desirable immune elicitations.

ACKNOWLEDGMENTS

We thank L. Yichen, Harvard AIDS Institute, Harvard University, and A. Schultz, NIAID, National Institutes of Health, for providing the SHIV strains and for their helpful discussions. We also thank J. Esparza and S. Osmanov, UNAIDS, Geneva, Switzerland; S. Beddows and J. Weber, Medical Research Council, London, United Kingdom; and Eva-Maria Fenyo, Microbiology and Tumorbiology Center Karolinska, Stockholm, Sweden, for their helpful discussions.

This work was supported by a grant-in-aid from the Ministry of Health and Welfare, Japan, and the Japan Health Sciences Foundation (grants 341-5 and 321-2).

REFERENCES

1. **Aldovini, A., and R. A. Young.** 1991. Humoral and cell-mediated immune responses to live recombinant BCG-HIV vaccines. Nature **351**:479–482.
2. **Amara, R. R., F. Villinger, J. D. Altman, S. L. Lydy, S. P. O'Neil, S. I. Staprans, D. C. Montefiori, Y. Xu, J. G. Herndon, L. S. Wyatt, M. A. Candido, N. L. Kozyr, P. L. Earl, J. M. Smith, H. L. Ma, B. D. Grimm, M. L. Hulsey, J. Miller, H. M. McClure, J. M. McNicholl, B. Moss, and H. L. Robinson.** 2001. Control of a mucosal challenge and prevention of AIDS by a multiprotein DNA/MVA vaccine. Science **292**:69–74.
3. **Baba, T. W., V. Liska, A. H. Khimani, N. B. Ray, P. J. Dailey, D. Penninck, R. Bronson, M. F. Greene, H. M. McClure, L. N. Martin, and R. M. Ruprecht.** 1999. Live attenuated, multiply deleted simian immunodeficiency virus causes AIDS in infant and adult macaques. Nat. Med. **5**:194–203.
4. **Baba, T. W., Y. S. Jeong, D. Pennick, R. Bronson, M. F. Greene, and R. M. Ruprecht.** 1995. Pathogenicity of live, attenuated SIV after mucosal infection of neonatal macaques. Science **267**:1820–1825.
5. **Barouch, D. H., S. Santra, J. E. Schmitz, M. J. Kuroda, T. M. Fu, W. Wagner, M. Bilska, A. Craiu, X. X. Zheng, G. R. Krivulka, K. Beaudry, M. A. Lifton, C. E. Nickerson, W. L. Trigona, K. Punt, D. C. Freed, L. Guan, S. Dubey, D. Casimiro, A. Simon, M. E. Davies, M. Chastain, T. B. Strom, R. S. Gelman, D. C. Montefiori, M. G. Lewis, E. A. Emini, J. W. Shiver, and N. L. Letvin.** 2000. Control of viremia and prevention of clinical AIDS in rhesus monkeys by cytokine-augmented DNA vaccination. Science **290**:486–492.
6. **Barouch, D. H., S. Santra, M. J. Kuroda, J. E. Schmitz, R. Plishka, A. Buckler-White, A. E. Gaitan, R. Zin, J. H. Nam, L. S. Wyatt, M. A. Lifton, C. E. Nickerson, B. Moss, D. C. Montefiori, V. M. Hirsch, and N. L. Letvin.** 2001. Reduction of simian-human immunodeficiency virus 89.6P viremia in rhesus monkeys by recombinant modified vaccinia virus Ankara vaccination. J. Virol. **75**:5151–5158.
7. **Bloom, B. R.** 1989. New approaches to vaccine development. Rev. Infect. Dis. **11**(Suppl. 2):S460–S466.
8. **Cecilia, D., V. N. KewalRamani, J. O'Leary, B. Volsky, P. Nyambi, S. Burda, S. Xu, D. R. Littman, and S. Zolla-Pazner.** 1998. Neutralization profiles of primary human immunodeficiency virus type 1 isolates in the context of coreceptor usage. J. Virol. **72**:6988–6996.
9. **Chujoh, Y., K. Matsuo, H. Yoshizaki, T. Nakasatomi, K. Someya, Y. Okamoto, S. Naganawa, S. Haga, H. Yoshikura, A. Yamazaki, S. Yamazaki, and M. Honda.** 2002. Cross-clade neutralizing antibody production against human immunodeficiency virus type 1 clade E and B′ strains by recombinant *Mycobacterium bovis* BCG-based candidate vaccine. Vaccine **20**:797–804.
10. **Earl, P. L., L. S. Wyatt, D. C. Montefiori, M. Bilska, R. Woodward, P. D. Markham, J. D. Malley, T. U. Vogel, T. M. Allen, D. I. Watkins, N. Miller, and B. Moss.** 2002. Comparison of vaccine strategies using recombinant *env-gag-pol* MVA with or without an oligomeric Env protein boost in the SHIV rhesus macaque model. Virology **294**:270–281.
11. **Falk, L. A., K. L. Goldenthal, J. Esparza, M. T. Aguado, S. Osmanov, W. R. Ballou, S. Beddows, N. Bhamarapravati, G. Biberfeld, G. Ferrari, D. Hoft, M. Honda, A. Jackson, Y. Lu, G. Marchal, J. McKinney, and S. Yamazaki.** 2000. Recombinant bacillus Calmette-Guerin as a potential vector for preventive HIV type 1 vaccines. AIDS Res. Hum. Retrovir. **16**:91–98.
12. **Feinberg, M. B., and J. P. Moore.** 2002. AIDS vaccine models: challenging challenge viruses. Nat. Med. **8**:207–210.
13. **Ghiara, J. B., E. A. Stura, R. L. Stanfield, A. T. Profy, and I. A. Wilson.** 1994. Crystal structure of the principal neutralization site of HIV-1. Science **264**: 82–85.
14. **Haynes, B. F., S. B. Putman, and J. B. Weinberg.** 1996. Update on the issues of HIV vaccine development. Ann. Med. **28**:39–41.
15. **Hiroi, T., H. Goto, K. Someya, M. Yanagita, M. Honda, N. Yamanaka, and H. Kiyono.** 2001. HIV mucosal vaccine: nasal immunization with rBCG-V3J1 induces a long term V3J1 peptide-specific neutralizing immunity in Th1- and Th2-deficient conditions. J. Immunol. **167**:5862–5867.
16. **Honda, M., K. Matsuo, T. Nakasone, Y. Okamoto, H. Yoshizaki, K. Kitamura, W. Sugiura, K. Watanabe, Y. Fukushima, S. Haga, Y. Katsura, H. Tasaka, K. Komuro, T. Tamada, T. Asano, A. Yamazaki, and S. Yamazaki.** 1995. Protective immune responses induced by secretion of a chimeric soluble protein from a recombinant *Mycobacterium bovis* bacillus Calmette-Guerin vector candidate vaccine for human immunodeficiency virus type 1 in small animals. Proc. Natl. Acad. Sci. USA **92**:10693–10697.
17. **Honda, M., S. Yamamoto, M. Cheng, K. Yasukawa, H. Suzuki, T. Saito, Y. Osugi, T. Tokunaga, and T. Kishimoto.** 1992. Human soluble IL-6 receptor: its detection and enhanced release by HIV infection. J. Immunol. **148**:2175–2180.
18. **Izumi, Y., Y. Ami, T. Nakasone, K. Matsuo, K. Someya, T. Sata, N. Yamamoto, and M. Honda.** 2003. Intravenous inoculation of replication-deficient recombinant vaccinia virus DIs expressing simian immunodeficiency virus Gag controls highly pathogenic simian-human immunodeficiency virus in monkeys. J. Virol. **77**:13248–13256.
19. **Jin, X., D. E. Bauer, S. E. Tuttleton, S. Lewin, A. Gettie, J. Blanchard, C. E. Irwin, J. T. Safrit, J. Mittler, L. Weinberger, L. G. Kostrikis, L. Zhang, A. S. Perelson, and D. D. Ho.** 1999. Dramatic rise in plasma viremia after $CD8^+$ T cell depletion in simian immunodeficiency virus-infected macaques. J. Exp. Med. **189**:991–998.
20. **Karlsson, G. B., M. Halloran, J. Li, I. W. Park, R. Gomila, K. A. Reimann, M. K. Axthelm, S. A. Iliff, N. L. Letvin, and J. Sodroski.** 1997. Characterization of molecularly cloned simian-human immunodeficiency viruses causing rapid $CD4^+$ lymphocyte depletion in rhesus monkeys. J. Virol. **71**:4218–4225.
21. **Kawahara, M., A. Hashimoto, I. Toida, and M. Honda.** 2002. Oral recombinant *Mycobacterium bovis* bacillus Calmette-Guerin expressing HIV-1 antigens as a freeze-dried vaccine induces long-term, HIV-specific mucosal and systemic immunity. Clin. Immunol. **105**:326–331.
22. **Kawahara, M., K. Matsuo, T. Nakasone, T. Hiroi, H. Kiyono, S. Matsumoto, T. Yamada, N. Yamamoto, and M. Honda.** 2002. Combined intrarectal/intradermal inoculation of recombinant *Mycobacterium bovis* bacillus Calmette-Guerin (BCG) induces enhanced immune responses against the inserted HIV-1 V3 antigen. Vaccine **21**:158–166.
23. **Kitsutani, P. T., S. Naganawa, T. Shiino, M. Matsuda, M. Honda, K. Yamada, M. Taki, and W. Sugiura.** 1998. HIV type 1 subtypes of nonhemophiliac patients in Japan. AIDS Res. Hum. Retrovir. **14**:1099–1103.
24. **Kuromatsu, I., K. Matsuo, S. Takamura, G. Kim, Y. Takebe, J. Kawamura, and Y. Yasutomi.** 2001. Induction of effective antitumor immune responses in a mouse bladder tumor model by using DNA of an alpha antigen from mycobacteria. Cancer Gene Ther. **8**:483–490.
25. **Letvin, N. L., D. H. Barouch, and D. C. Montefiori.** 2002. Prospects for vaccine protection against HIV-1 infection and AIDS. Annu. Rev. Immunol. **20**:73–99.
26. **Letvin, N. L., S. Robinson, D. Rohne, M. K. Axthelm, J. W. Fanton, M. Bilska, T. J. Palker, H. X. Liao, B. F. Haynes, and D. C. Montefiori.** 2001. Vaccine-elicited V3 loop-specific antibodies in rhesus monkeys and control of a simian-human immunodeficiency virus expressing a primary patient human immunodeficiency virus type 1 isolate envelope. J. Virol. **75**:4165–4175.
27. **Liao, H. X., B. Etemad-Moghadam, D. C. Montefiori, Y. Sun, J. Sodroski, R. M. Scearce, R. W. Doms, J. R. Thomasch, S. Robinson, N. L. Letvin, and B. F. Haynes.** 2000. Induction of antibodies in guinea pigs and rhesus monkeys against the human immunodeficiency virus type 1 envelope: neutralization of nonpathogenic and pathogenic primary isolate simian/human immunodeficiency virus strains. J. Virol. **74**:254–263.
28. **Lifson, J. D., and M. A. Martin.** 2002. One step forwards, one step back. Nature **415**:272–273.
29. **Lu, Y., M. S. Salvato, C. D. Pauza, J. Li, J. Sodroski, K. Manson, M. Wyand, N. Letvin, S. Jenkins, N. Touzjian, C. Chutkowski, N. Kushner, M. LeFaile, L. G. Payne, and B. Roberts.** 1996. Utility of SHIV for testing HIV-1 vaccine candidates in macaques. J. Acquir. Immune Defic. Syndr. Hum. Retrovirol. **12**:99–106.
30. **Matsumoto, S., M. Tamaki, H. Yukitake, T. Matsuo, M. Naito, H. Teraoka, and T. Yamada.** 1996. A stable *Escherichia coli*-mycobacteria shuttle vector 'pSO246' in *Mycobacterium bovis* BCG. FEMS Microbiol. Lett. **135**:237–243.
31. **McCune, J. M.** 2001. The dynamics of $CD4^+$ T-cell depletion in HIV disease. Nature **410**:974–979.
32. **Mori, K., Y. Yasutomi, S. Ohgimoto, T. Nakasone, S. Takamura, T. Shioda, and Y. Nagai.** 2001. Quintuple deglycosylation mutant of simian immunodeficiency virus SIVmac239 in rhesus macaques: robust primary replication, tightly contained chronic infection, and elicitation of potent immunity against the parental wild-type strain. J. Virol. **75**:4023–4028.
33. **Mothe, B. R., H. Horton, D. K. Carter, T. M. Allen, M. E. Liebl, P. Skinner, T. U. Vogel, S. Fuenger, K. Vielhuber, W. Rehrauer, N. Wilson, G. Franchini, J. D. Altman, A. Haase, L. J. Picker, D. B. Allison, and D. I. Watkins.** 2002. Dominance of CD8 responses specific for epitopes bound by a single major histocompatibility complex class I molecule during the acute phase of viral infection. J. Virol. **76**:875–884.

34. **Musey, L., J. Hughes, T. Schacker, T. Shea, L. Corey, and M. J. McElrath.** 1997. Cytotoxic-T-cell responses, viral load, and disease progression in early human immunodeficiency virus type 1 infection. N. Engl. J. Med. **337**:1267–1274.
35. **Nabel, G., W. Makgoba, and J. Esparza.** 2002. HIV-1 diversity and vaccine development. Science **296**:2335.
36. **Nabel, G. J.** 2002. HIV vaccine strategies. Vaccine **20**:1945–1947.
37. **Nishimura, Y., T. Igarashi, N. Haigwood, R. Sadjadpour, R. J. Plishka, A. Buckler-White, R. Shibata, and M. A. Martin.** 2002. Determination of a statistically valid neutralization titer in plasma that confers protection against simian-human immunodeficiency virus challenge following passive transfer of high-titered neutralizing antibodies. J. Virol. **76**:2123–2130.
38. **Ogg, G. S., X. Jin, S. Bonhoeffer, P. R. Dunbar, M. A. Nowak, S. Monard, J. P. Segal, Y. Cao, S. L. Rowland-Jones, V. Cerundolo, A. Hurley, M. Markowitz, D. D. Ho, D. F. Nixon, and A. J. McMichael.** 1998. Quantitation of HIV-1-specific cytotoxic T lymphocytes and plasma load of viral RNA. Science **279**:2103–2106.
39. **Okamoto, Y., Y. Eda, A. Ogura, S. Shibata, T. Amagai, Y. Katsura, T. Asano, K. Kimachi, K. Makizumi, and M. Honda.** 1998. In SCID-hu mice, passive transfer of a humanized antibody prevents infection and atrophic change of medulla in human thymic implant due to intravenous inoculation of primary HIV-1 isolate. J. Immunol. **160**:69–76.
40. **Ota, M. O., J. Vekemans, S. E. Schlegel-Haueter, K. Fielding, M. Sanneh, M. Kidd, M. J. Newport, P. Aaby, H. Whittle, P. H. Lambert, K. P. McAdam, C. A. Siegrist, and A. Marchant.** 2002. Influence of *Mycobacterium bovis* bacillus Calmette-Guerin on antibody and cytokine responses to human neonatal vaccination. J. Immunol. **168**:919–925.
41. **Reimann, K. A., J. T. Li, R. Veazey, M. Halloran, I. W. Park, G. B. Karlsson, J. Sodroski, and N. L. Letvin.** 1996. A chimeric simian/human immunodeficiency virus expressing a primary patient human immunodeficiency virus type 1 isolate *env* causes an AIDS-like disease after in vivo passage in rhesus monkeys. J. Virol. **70**:6922–6928.
42. **Robinson, H. L.** 2002. New hope for an AIDS vaccine. Nat. Rev. Immunol. **2**:239–250.
43. **Roche, P. W., P. W. Peake, H. Billman-Jacobe, T. Doran, and W. J. Britton.** 1994. T-cell determinants and antibody binding sites on the major mycobacterial secretory protein MPB59 of *Mycobacterium bovis*. Infect. Immun. **62**:5319–5326.
44. **Sasaki, Y., Y. Ami, T. Nakasone, K. Shinohara, E. Takahashi, S. Ando, K. Someya, Y. Suzaki, and M. Honda.** 2000. Induction of CD95 ligand expression on T lymphocytes and B lymphocytes and its contribution to apoptosis of CD95-up-regulated CD4$^+$ T lymphocytes in macaques by infection with a pathogenic simian/human immunodeficiency virus. Clin. Exp. Immunol. **122**:381–389.
45. **Schmitz, J. E., M. J. Kuroda, S. Santra, V. G. Sasseville, M. A. Simon, M. A. Lifton, P. Racz, K. Tenner-Racz, M. Dalesandro, B. J. Scallon, J. Ghrayeb, M. A. Forman, D. C. Montefiori, E. P. Rieber, N. L. Letvin, and K. A. Reimann.** 1999. Control of viremia in simian immunodeficiency virus infection by CD8$^+$ lymphocytes. Science **283**:857–860.
46. **Shibata, R., T. Igarashi, N. Haigwood, A. Buckler-White, R. Ogert, W. Ross, R. Willey, M. W. Cho, and M. A. Martin.** 1999. Neutralizing antibody directed against the HIV-1 envelope glycoprotein can completely block HIV-1/SIV chimeric virus infections of macaque monkeys. Nat. Med. **5**:204–210.
47. **Shinohara, K., K. Sakai, S. Ando, Y. Ami, N. Yoshino, E. Takahashi, K. Someya, Y. Suzaki, T. Nakasone, Y. Sasaki, M. Kaizu, Y. Lu, and M. Honda.** 1999. A highly pathogenic simian/human immunodeficiency virus with genetic changes in cynomolgus monkey. J. Gen. Virol. **80**:1231–1240.
48. **Someya, K., K. Q. Xin, K. Matsuo, K. Okuda, N. Yamamoto, and M. Honda.** 2004. A consecutive prime-boost vaccination of mice with simian immunodeficiency virus (SIV) *gag/pol* DNA and recombinant vaccinia virus strain DIs elicits effective anti-SIV immunity. J. Virol. **78**:8942–8953.
49. **Stover, C. K., V. F. de la Cruz, T. R. Fuerst, J. E. Burlein, L. A. Benson, L. T. Bennett, G. P. Bansal, J. F. Young, M. H. Lee, G. F. Hatfull, S. B. Snapper, R. G. Barletta, W. R. Jacobs, Jr., and B. R. Bloom.** 1991. New use of BCG for recombinant vaccines. Nature **351**:456–460.
50. **Weiss, R. A.** 2002. HIV receptors and cellular tropism. IUBMB Life **53**:201–205.
51. **Wu, S. C., J. L. Spouge, S. R. Conley, W. P. Tsai, M. J. Merges, and P. L. Nara.** 1995. Human plasma enhances the infectivity of primary human immunodeficiency virus type 1 isolates in peripheral blood mononuclear cells and monocyte-derived macrophages. J. Virol. **69**:6054–6062.
52. **Yamanaka, T., Y. Fujimura, S. Ishimoto, A. Yoshioka, M. Konishi, N. Narita, J. Mimaya, T. Meguro, T. Nakasone, Y. Okamoto, H. Yoshizaki, K. Yamada, and M. Honda.** 1997. Correlation of titer of antibody to principal *neutralizing* domain of HIVMN strain with disease progression in Japanese hemophiliacs seropositive for HIV type 1. AIDS Res. Hum. Retrovir. **13**:317–326.
53. **Ye, Y., Z. H. Si, J. P. Moore, and J. Sodroski.** 2000. Association of structural changes in the V2 and V3 loops of the gp120 envelope glycoprotein with acquisition of neutralization resistance in a simian-human immunodeficiency virus passaged in vivo. J. Virol. **74**:11955–11962.
54. **Zhang, Y., B. Lou, R. B. Lal, A. Gettie, P. A. Marx, and J. P. Moore.** 2000. Use of inhibitors to evaluate coreceptor usage by simian and simian/human immunodeficiency viruses and human immunodeficiency virus type 2 in primary cells. J. Virol. **74**:6893–6910.

Available online at www.sciencedirect.com
SCIENCE DIRECT®
Biochemical and Biophysical Research Communications 320 (2004) 544–550
BBRC
www.elsevier.com/locate/ybbrc

Intracellular expression of antisense RNA transcripts complementary to the human immunodeficiency virus type-1 *vif* gene inhibits viral replication in infected T-lymphoblastoid cells

Jacob Samson Barnor,[a,d] Naoko Miyano-Kurosaki,[a,b] Kazuya Yamaguchi,[a] Atsushi Sakamoto,[a] Koichi Ishikawa,[c] Yoshio Inagaki,[e] Naoki Yamamoto,[c,e] Mubarak Osei-Kwasi,[d] David Ofori-Adjei,[d] and Hiroshi Takaku[a,b,*]

[a] *Department of Life and Environmental Science, 2-17-1 Tsudanuma, 275-0016 Narashino, Chiba, Japan*
[b] *High Technology Research Center, Chiba Institute of Technology, 2-17-1 Tsudanuma, 275-0016 Narashino, Chiba, Japan*
[c] *National Institute of Infectious Diseases, AIDS Research Center, Japan*
[d] *Department of Virology, Noguchi Memorial Institute for Medical Research, Accra-Ghana*
[e] *Tokyo Medical and Dental University, Japan*

Received 20 April 2004

Abstract

The human immunodeficiency virus type-1 (HIV-1)-encoded *vif* protein is essential for viral replication, virion production, and pathogenicity. HIV-1 *vif* interacts with the endogenous human APOBEC3G protein (an mRNA editor) in target cells to prevent its virions from encapsidation. Although some studies have established targets within the HIV-1 *vif* gene that are important for its biologic function, it is however important to further screen for effective therapeutic targets in the *vif* gene that could interfere with the HIV-1 *vif*-dependent infectivity and pathogenicity. This report demonstrates that HIV-1 *vif* antisense RNA fragments constructed within mid-3′ region, notably the region spanning nucleic acid positions 5561–5705 (M-3′-AS), significantly inhibited HIV-1 replication in MT-4 and H9-infected cells and reduced the HIV-1 *vif* mRNA transcripts. These data clearly suggest that the above *vif* fragment, which corresponds to amino acid residues 96–144, could be an effective novel therapeutic target site for gene therapy applications, for the control and management of HIV-1 infection, due to its strong inhibition of HIV-1 replication in cells.
© 2004 Elsevier Inc. All rights reserved.

Keywords: HIV-1 *vif*; Antisense RNA; Inhibition of HIV-1 replication; Gene therapy

Human immunodeficiency virus type-1 (HIV-1) encodes six accessory proteins, *vpr*, *vpu*, *nef*, *rev*, *tat*, and *vif*, apart from its major structural *gag-pol* and *env* proteins. The *vif* protein is well conserved in all lentiviruses, except for the equine infectious anemia virus [1]. The *vif*-conserved lentiviruses include feline immunodeficiency virus, caprine arthritis encephalitis virus, bovine immunodeficiency virus, and simian immunodeficiency virus [2–4]. The HIV-1 *vif* gene encodes a highly basic, 23,000-M_r phosphoprotein that collapses intermediate filaments, localizes in the cytoplasm of its infected target cells, and acts during virus assembly by an unknown mechanism to enhance viral infectivity [5–9]. HIV-1 *vif* is viral- and cellular-specific [10,11], and is therefore critically essential for cells designated as non-permissive, such as H9, CEM, and U38, and is non-critical for cells classified as permissive, such as HeLa-CD4$^+$, SupT1, COS, MT-4, and Jurkat cells [12,13]. HIV-1 *vif* does not influence the expression or incorporation of the major encoded structural proteins. Hence, various studies have demonstrated that components such as viral proteins and nucleic acids were not changed in virions generated in non-permissive

* Corresponding author. Fax: +81-47-471-8764.
E-mail address: takaku@ic.it-chiba.ac.jp (H. Takaku).

0006-291X/$ - see front matter © 2004 Elsevier Inc. All rights reserved.
doi:10.1016/j.bbrc.2004.05.201

cells [14]. Recently, it had been demonstrated that CEM 15, now known as (APOBEC3G), which is only expressed in non-permissive cells [15,16], is that endogenous inhibitor. When expressed in permissive cells, APOBEC3G makes the cells non-permissive. It is proposed to act in concert with other cellular factors such as sp 140 [17]. The function of APOBEC3G is similar to that of APOBEC-1 (apoB mRNA editing catalytic subunit 1), a cytidine deaminase that converts cytidine into uridine in the mRNA of apolipoprotein B [18].

Simon et al. [19] determined that every amino acid position dispersed throughout the linear sequence of *vif* is important for *vif* function, because all the amino acid positions analyzed in their scanning mutation studies of the *vif* protein either decreased or increased infectivity. Therefore, we hypothesized that targeting the profile of the HIV-1 *vif* gene with anti-HIV-1 gene molecules could result in novel target sites that might be useful for HIV gene therapy applications. Gene therapy has recently emerged as a promising therapeutic tool for the treatment of genetic diseases, cancers, and chronic infectious conditions, such as AIDS [20]. These include the intracellular expression of decoy RNAs, ribozymes, single-chain antibodies, *trans*-dominant proteins, and antisense RNAs. To date, antisense RNAs and other anti-HIV RNA molecules targeted to various HIV-1 major structural genes, accessory genes, and receptors successfully inhibited viral replication in the target cells. [21–36].

In the present study, we constructed HIV-1 *vif* antisense RNA expression vectors of various sizes to screen the *vif* gene for novel site(s) that will mediate attenuation of the *vif*-dependent infectivity in the cells, and some experiments were controlled by *gag* and *env* antisense RNA previously described by Park et al. [37]. The potential anti-HIV-1 efficacies of these HIV-1 *vif* antisense RNA molecules were evaluated for their suitability of becoming effective therapeutic target(s) for HIV gene therapy applications for the control and management of HIV-AIDS.

Materials and methods

Cell cultures. COS, HeLa-CD4$^+$, H9, and MT-4 cells were grown in complete culture medium consisting of either RPMI 1640 medium (Sigma Chemical, St. Louis, MO) or DMEM (Gibco, Invitrogen, Japan) supplemented with 10% (v/v) heat-inactivated fetal bovine serum (FBS), L-glutamine (2 mM), penicillin (100 U/ml), and streptomycin (100 μg/ml). All cultures were maintained at 37 °C under a 5% CO_2 atmosphere.

Construction of HIV-1 vif antisense RNA expression vectors and generation of virus vector. HIV-1 *vif* antisense and sense RNA expression vectors based on the eukaryotic vector pcDNA3.1 (+/−) (Invitrogen, Japan) were constructed. The various target sites of the *vif* gene were amplified from pNLE HIV-1 by PCR using KOD plus polymerase with the forward and reverse primers containing the *Eco*RV and *Xho*I recognition sites, respectively. (i) For the *vif*-ORF antisense RNA (*vif*-AS), which extended from nucleotide positions 5271 to 5849, the *forward primer* was V-FecoV: (5′-GAT ATC ATG GAA AAC AGA TGG CAG GTG ATG-3′) and the *reverse primer* V-Rxho: (5′-CTC GAG CTA GTG TCC ATT CAT TGT ATG GCT-3′); (ii) for the 5′-*vif* antisense RNA (5′-AS), (5271–5560), the *forward primer* was the same as V-FecoV and the *reverse primer* V-MRXho; (5′-CTC GAG TGT GTG CTA TAT CTC TTT TTC CTC-3′); (iii) for the mid-*vif* (M-AS), (5417–5560) the *forward primer* was V-4FecoV: (5′-GAT ATC CAA AAA TAA GTT CAG AAG TAC ACA TCC C-3′) and was paired with the *reverse primer* V-4RXho: (5′-CTC GAG TAG AGA TCC TAC CTT GTT ATG TCC TGC C-3′); and (iv) for the 3′-*vif*, (3′-AS): (5561–5849) the *forward primer* was V-MFecoV: (5′-GAT ATC AGT AGA CCC TGA CCT AGC AGA CC-3′) paired with the *reverse primer* V-Rxho. Similarly, the short *vif* antisense RNA fragments were generated with the following sets of primers: (v) for the M-5′ *vif* antisense RNA (M-5′-AS), (5417–5560), the *forward primer* was V-4FecoV and the *reverse primer* was V-4Rxho (5′-CTC GAG TGT GTG CTA TAT CTC TTT TTC CTC-3′); (vi) for the Mid-Mid *vif* antisense RNA (M-M-AS), (5488–5632), the *forward primer* was V-4MFecoV (5′-GAT ATC ATA CAG GAG AAA GAG ACT GGC AT-3′), and the *reverse primer* was V-4MRXho: (5′-CTC GAG CTT ATA GCA GAT TCT GAA AAA CAA TCA AAA TA-3′); (vii) for the Mid-3′ *vif* antisense RNA (M-3′-AS), (5561–5705), the *forward primer* was the same as V-MFecoV and the *reverse primer* was the same as V-4MRXho; (viii) while the *forward primer* for the 3′-Mid *vif* antisense RNA (3′-M-AS), (5633–5778) was V-3′ MFecoV (5′-GAT ATC AAT ACC ATA TTA GGA CGT ATA GTT AGT CC-3′) and the *reverse primer* was V-3MRXho: (5′-CTC GAG TCA GTT TCC TAA CAC TAG GCA AAG GTG GCT-3′); (ix) finally, the set of primers for the 3′–3′ *vif* antisense RNA (3′–3′-AS) (5706–5849) as follows: the *forward primer* was V-3FecoV: (5′-GAT ATC CAG TAC TTG GCA CTA GCA GCA TTA-3′) and the *reverse primer* was V-RXho. The PCRs were performed according to the manufacturers' protocols, and the integrity of the resulting *vif* fragments was confirmed by automated sequencing. These amplified fragments were then cloned into the *Eco*RV and *Xho*I sites in the pcDNA3.1 (+/−) vector in both the antisense and sense orientations, to generate the *vif* antisense RNA and the control sense expression vectors. The sense and antisense RNA of HIV-1 *gag* (G1) and *env* (E2) fragments extending from nucleotide positions 1564–2010 and 7070–8186 of pNL4-3, respectively, were further used as controls in some experiments [37]. We used the pNLE HIV-1 infectious molecular clone [38], which was based on the previously described pNL4-3 HIV-1, to generate the virus vector [39]. Harvesting cell-free virus from the supernatant of transfected HeLa-CD4$^+$ or H9 cells generated the wild-type (wt) HIV-1_{NLE} used in the infection assays.

Transfections. The HIV-1 *vif* antisense RNA vectors including the env and gag vectors (control for some experiments) were either separately transfected or co-transfected with pNLE HIV-1 into COS (3×10^5), HeLa-CD4$^+$ (2×10^5), or H9 at 5×10^5 cells per 60-mm culture dish, using FuGENE 6 transfection reagent (Roche Diagnostics, Japan) and Lipofectamine 2000 (Life Technologies, Japan) according to the manufacturers' protocols. Briefly, 24 h before transfection, the adherent cells were seeded as described above. COS and HeLa-CD4$^+$ cells were transfected with 3.0 μg antisense vector DNA or co-transfected with 2 μg antisense DNA and 2 μg pNLE HIV-1 DNA using 3 μl FuGENE 6 reagent. H9 cells were transfected with 3 μl Lipofectamine 2000 transfection reagent, optimized with 50 μl serum-free Opti-MEM. After 72 h of culture, the supernatants were harvested and cleared by centrifugation, and HIV-1 *gag* p24 antigen production was measured using an enzyme-linked immunosorbent assay system (CLEIA) [40]. The remaining cells were washed and fixed in 1% formaldehyde in phosphate-buffered saline. The co-transfected cells were subsequently monitored for down-regulation of the expressed reporter gene (EGFP) using fluorescence microscopy.

RNA extraction and intracellular expression of vector and viral mRNAs. Total cellular RNA was isolated from transfected and co-transfected COS cells with the GenElute Mammalian Total RNA Kit (Sigma Chemical), according to the manufacturer's instructions. The isolated RNA samples were pretreated with DNase I (Promega) and then subjected to one-step RT-PCR assays (RT-PCR high-plus-kit; Toyobo, Japan) with specific HIV-1 *vif* mRNA detection primers, *forward primer*: vmRNA-F, (5′-CAA GAA GAA AAG CAA AGA TCA TCA G-3′) and *reverse primer*: vmRNA-R, (5′-CTA GTG TCC ATT CAT TGT ATG GCT-3′), according to the manufacturer's instructions. Briefly, the RNA samples were normalized at 1 μg per reaction and concomitantly amplified with G3PDH as an internal control. To analyze the extent of the RNA expression in the cells, the products from the RT-PCR amplified RNAs were electrophoresed through a non-denaturing 1.8% agarose gel in TAE buffer.

Effect of HIV-1 antisense RNAs on viral infectivity. To evaluate the antisense effect on the replication competencies of the HIV-1 virions, stock viruses from multiple samples generated from co-transfected H9 cells were further normalized at 100 pg of HIV-1 *gag* p24 antigen equivalents each and assayed for replication competency using the terminal dilution micro-assay in susceptible MT-4 cells. End-point titration was performed in flat-bottomed micro-titer wells using four parallel series of fivefold dilutions. After 5–7 days of incubation, cell-free supernatants were harvested and the presence of the major viral core p24 protein was examined using an HIV-1 p24 CLEIA. The $TCID_{50}$ was calculated by the method of Reed and Muench [41]. The result was presented as mean ± SD of three independent experiments.

Time course of HIV-1 infection inhibition in H9 cells by HIV-1 vif antisense M-3′-AS. H9 cells (2×10^5) were transfected 24 h before infection with HIV-i_{NLE} (100 pg p24 antigen) with 2 μg vector DNA (M-3′-AS, and M-3′-S) using Lipofectamine 2000 according to the manufacturer's directions. Sixteen hours after infection, cells were washed to remove residual virus and then cultured in medium containing 1% FBS. Cell-free supernatant was sampled from culture medium over a period of days 2, 6, 10, and 14, and monitored for p24 antigen using an HIV-1 p24 CLEIA.

Results and discussion

Intracellular expression of antisense mRNAs in the cells

The target sites used in this study for the construction of the HIV-1 *vif* antisense RNA expression vectors are schematically represented in Fig. 1B, which were based on the HIV-1 pNLE genome (Fig. 1A). The HIV-1 *vif* antisense RNA expression vectors, hereafter referred to as the *vif*-AS (5271–5849), 5′-AS (5271–5560), M-AS (5417–5705), and 3′-AS (5561–5849) vectors, were each approximately 288 bp designated as long antisense vectors. The M-5′-AS (5417–5560), M-M-AS (5488–5632), M-3′-AS (5561–5705), 3′-M-AS (5633–5778), and 3′–3′-AS (5706–5849) vectors were designated as short *vif* antisense RNA expression vectors and were approximately 145 bp each (Fig. 1B).

Since the antisense mechanism is partly dependent on the expressed antisense mRNA in the cells, and their accessibility of the target mRNA, we determined the level of expressed mRNA for all the antisense RNA constructs in transiently transfected HeLa-CD4$^+$ cells. The following primer pair was used to amplify total RNA from co-transfected cells; *forward primer* vmRNA-F, (5′-CAA GAA GAA AAG CAA AGA TCA TCA G-3′) and reverse primer vmRNA-R, (5′-CTA GTG TCC ATT CAT TGT ATG GCT-3′). We observed the expression of both the antisense and sense mRNA in the cells (Figs. 1C-i and ii). Thus, warranting a comparative assessment of the inhibitory efficacies that

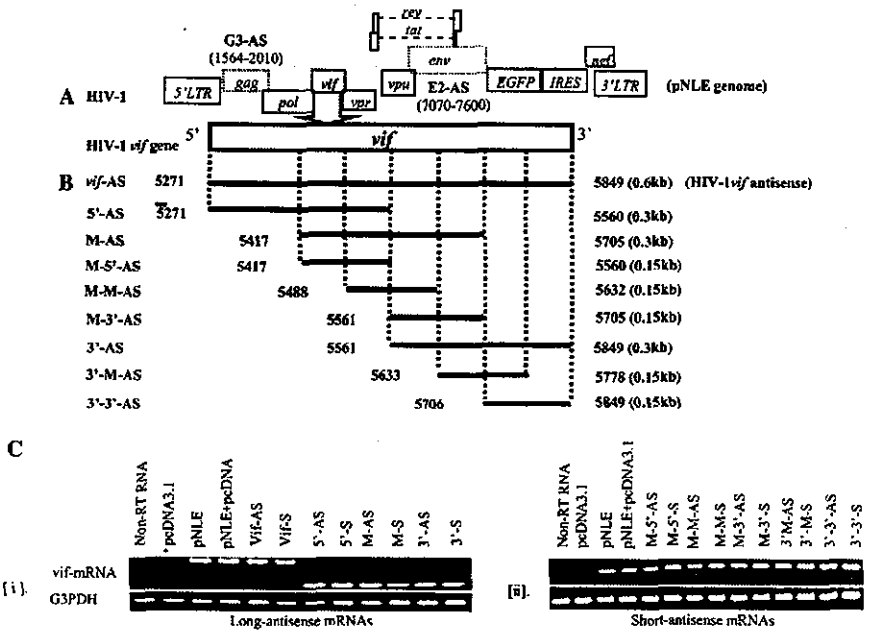

Fig. 1. Scheme for the construction of the HIV-1 *vif* antisense RNA expression vectors. (A) Schematic representation of the HIV-1 pNLE genome, showing the open reading frames, and the 5′ and 3′ long terminal repeats. (B) The selected *vif* targets were amplified by PCR, with added *Eco*RV and *Xho*I cloning sites and then ligated into the *Eco*RV and *Xho*I cloning site of pcDNA3.1 vector. (C-i.) RT-PCR analysis of expressed long-*vif* antisense mRNAs. (C-ii.) Expressed short-*vif* vector mRNAs in transfected HeLa CD4$^+$ cells, resolved on 1.8% agarose gel.

will be mediated by both antisense and sense RNA on the viral mRNAs in the cells.

RNA content and HIV-1 vif viral mRNA down-regulation

To determine the relative inhibitory efficacies between the long and short *vif* antisense RNA expression vectors, they were co-transfected with the pNLE HIV-1. The co-transfected vectors were examined for the down-regulation of the viral *vif* mRNA and the reporter gene expression. Total RNA isolated from the co-transfected HeLa-CD4$^+$ cells was concurrently amplified with an internal control RNA (G3PDH) and a non-RT subjected control by RT-PCR using the specific *vif* viral mRNA detection primers and the following pair of specific primers for the control RNA G3PDH. The *G3PDH-forward primer*: (5′-ACC ACA GTC CAT GCC ATC AC-3′) and the *G3PDH-reverse primer*: (5′-TCC ACC ACC CTG TTG CTG TA-3′). The long *vif* antisense RNA transcripts expressed by the vectors *vif*-AS, M-AS, and 3′-AS vectors (Fig. 2A; lanes 5, 9, and 11, respectively) mediated down-regulation of pNLE HIV-1 *vif* viral mRNA expression as compared with that of the control HIV-1 pNLE *vif* mRNA alone (lane 3). Similarly, the short *vif* antisense RNA expression vectors encoding the M-3′-AS and 3′-M-AS also mediated the down-regulation of HIV-1 pNLE *vif* mRNA

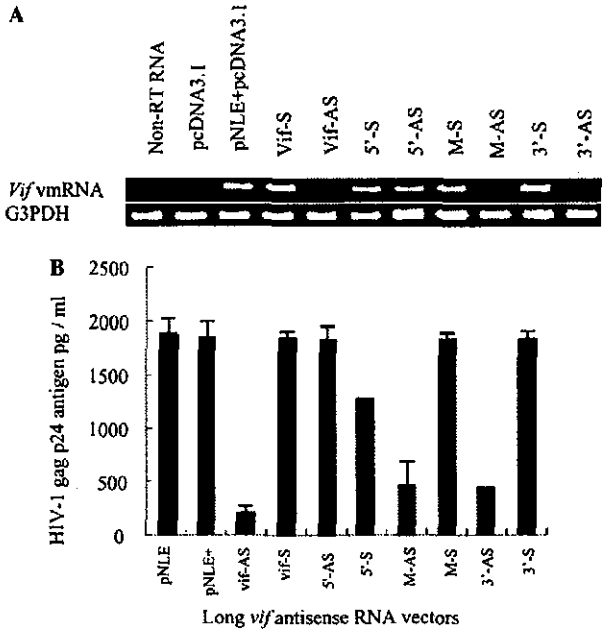

Fig. 2. Inhibition of HIV-1 viral *vif* mRNA and HIV-1 *gag* p24 antigen down-regulation. (A) RNA extracted from HeLa CD4$^+$ cells co-transfected with 3 μg long-*vif* antisense DNA and 2 μg pNLE HIV-1 DNA was subjected to RT-PCR and fractionated on a 1.8% agarose gel. (B) HIV-1 *gag* p24 antigen measured from harvested cell-free supernatants after 72 h culture by CLEIA. Data represent means ± SD of three independent experiments.

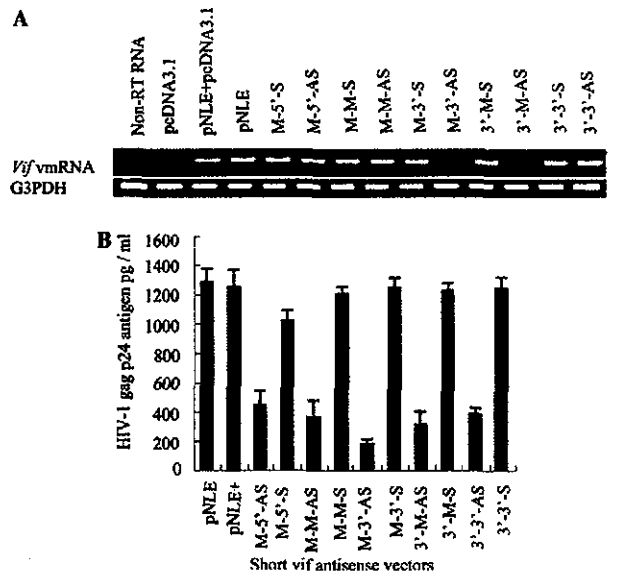

Fig. 3. Inhibition of HIV-1 viral *vif* mRNA and HIV-1 *gag* p24 antigen down-regulation. (A) RNA extracted from HeLa CD4$^+$ cells co-transfected with 3 μg short-*vif* antisense DNA and 2 μg pNLE HIV-1 DNA was subjected to RT-PCR and analyzed on a 1.8% agarose gel. (B) HIV-1 *gag* p24 antigen was measured from harvested cell-free supernatants after 72 h culture by CLEIA. Data represent means ± SD of three independent experiments.

expression (Fig. 3A; lanes 10 and 12) in comparison with the control HIV-1 pNLE *vif* mRNA alone (lane 4) and the control HIV-1 plus the empty vector (lane 3). Visualizing the RT-PCR products in ethidium-bromide-stained agarose gels thus provided a partial quantitative estimate of the degree of the reduction in the expressed HIV-1 *vif* viral mRNA. Although this method has no quantitative power in the real sense, the reduction was quite distinct to allow visual comparison. These reductions in the viral mRNA could be a result of the effective antisense mechanism mediated by the highly expressed *vif* antisense mRNA transcripts in the cells (Figs. 1C-i and ii).

HIV-1 gag p24 antigen production and as marker for the down-regulation of HIV-1 replication and infectivity

To determine the level of down-regulation in the HIV-1 *gag* p24 antigen production mediated by the expressed *vif* antisense RNAs, cell-free culture supernatants were harvested 72 h post-transfection and the remaining cells were observed under a fluorescence microscope to detect EGFP expression. The HIV-1 *gag* p24 antigen in the supernatant was measured using a fully automated CLEIA. The results exhibited varied levels of HIV-1 *gag* p24 antigen production in the cells by both the long- and short-*vif* antisense RNA vectors (Figs. 2B and 3B). Furthermore, equal concentrations of the HIV-1 virions derived from the co-transfected HeLa

CD4+ or H9 cells were normalized at 100 pg HIV-1 *gag* p24 antigen and titrated for infectivity by an endpoint micro-method in MT-4 or H9 cells in three independent experiments in 96-well plates (data are presented as means ± SD of three independent experiments). The infectivity titers were expressed as tissue culture infectivity dose 50 ($TCID_{50}$) per milliliter, and represent the highest virus dilution for which the HIV-1 *gag* p24 antigen was detected in 50% of the wells 7 days after infection. The results suggest defective virion production, from virions derived from H9 cells and further titrated on H9 cell (Figs. 4A and B). These results paralleled the level of down-regulation in the reporter gene expression (data not shown). Nevertheless, there was a correlation between the levels of HIV-1 *gag* p24 antigen production (Figs. 2B and 3B), the down-regulation of the HIV-1 *vif* mRNA 1 (Figs. 2A and 3A), and the down-regulation of the level of EGFP expression in the cells amongst these vectors (data not shown).

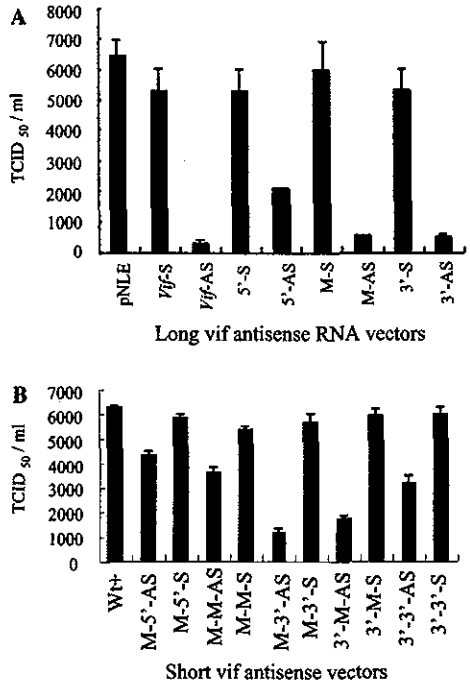

Fig. 4. Antisense RNAs mediated low infectivity on H9 cells. Antisense vector DNA (2 μg) was co-transfected with pNLE HIV-1 DNA (2 μg) in the presence of FuGENE 6 into HeLa CD4 and H9 cells. (A) HIV-1 virions derived from the long-*vif* antisense co-transfected cells were normalized at 100 pg HIV-1 *gag* p24 antigen and then titrated on MT-4 cells or H9 in fivefold serial dilution steps. (B) HIV-1 virions derived from the short-vif antisense co-transfected cells were normalized at 100 pg HIV-1 *gag* p24 antigen and then titrated on MT-4 cells or H9 in fivefold serial dilution steps. The HIV-1 *gag* p24 antigen was measured after 7 days of culture and the titer is expressed as $TCID_{50}$/ml. Data represent means ± SD of three independent experiments.

Efficacy of M-3′-AS against HIV-1 replication in H9 cells

To further elucidate the inhibition efficacy on HIV-1 replication, the M-3′-AS vector encoding the *vif* fragment 5561–5705, and the control gag (G3) and env (E2) antisense RNAs were co-transfected with pNLE HIV-1 in H9 cells. Comparative analysis of the HIV-1 *gag* p24 production level performed 72 h post-transfection revealed an increased inhibition of HIV-1 replication mediated by M-3′-AS compared to the G3 and E2 antisense RNA vectors, respectively (Fig. 5A).

The M-3′-AS vector mediated time course inhibition of HIV-1 replication

A time course inhibition assay was performed to further examine the inhibitory capacity of the M-3′-AS vector in relation with time. The M-3′-S and M-3′-AS vectors were transfected into H9 cells. The cells were subsequently challenged by infection with $HIV\text{-}1_{NLE}$

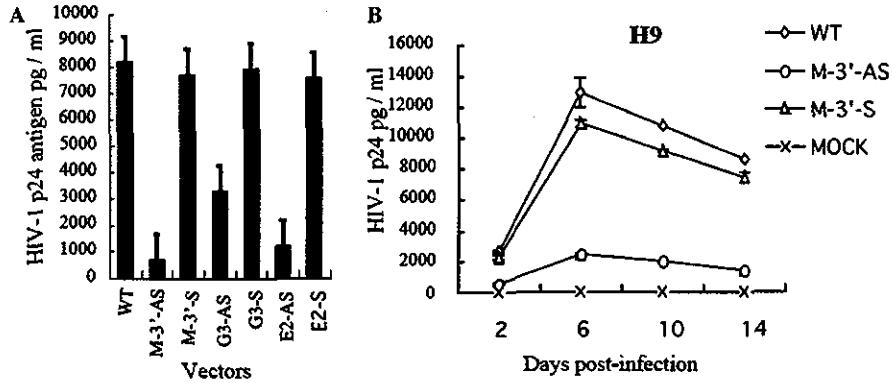

Fig. 5. Comparative efficacy of M-3′-AS and time-course inhibition of HIV-1 replication. H9 cell were co-transfected with 2 μg wt and 3 μg M-3′-AS, M-3′-S, and the *gag* (G3), and *env* (E2), respectively. (A) HIV-1 p24 assay was measured from cell-free culture supernatant by CLEIA after 72 h. (B) H9 cells were transfected with 2 μg M-3′-AS, control M-3′-S, and the empty vectors for 24 h, then cells were challenged with normalized 100 pg p24 antigen, and residual virus was removed after 6 h. HIV-1 *gag* p24 was measured in a time-course manner for 14 days. Data represent means ± SD of three independent experiments.

(100 pg p24) 24 h post-transfection. Six hours after infection, the cells were washed and further cultured for 14 days and then analyzed for HIV-1 *gag* p24 antigen production at various time points. There was high level of inhibition of HIV-1 replication in the infected H9 cells mediated by M-3′-AS over time, as compared to the sense and wt (Fig. 5B). In this study, we screened for highly effective therapeutic targets in the HIV-1 *vif* gene that interfered with the *vif*-dependent infectivity, due to the critical role *vif* has in the infectivity and pathogenicity in the target cells. The observed expression level and fidelity of the AS mRNA in the cells were high, which might have triggered sequence-specific antisense down-regulation of the HIV-1 *vif* mRNA in the co-transfected HeLa-CD4$^+$ cells, since expression and accessibility of the target mRNA are the key steps in the antisense mechanism. Nevertheless, others have shown that sequences and particularly that of the 3′ half of *vif*, downstream of splicing accepter (SA-#3 at nt 5463), are in multiple viral RNAs such as the genomic RNA and the RNAs encoding for *vif*, *vpr*, *tat*, *rev*, and *env*. Therefore, most likely triggering degradation or blocking the encapsidation of the viral genomic RNA or targeting multiple viral RNAs and therefore mediating multiple down-regulation of *tat*, *rev*, and *env*, and most likely triggering degradation or blocking the encapsidation of the viral genomic RNA [42]. However, our target that corresponded to the referred *vif* target M-5′-AS (5417–5560) did not mediate inhibition as high as the Mid-3′ *vif* antisense RNA (M-3′-AS), (5561–5705). Therefore making the site a novel *vif* target worth considering for HIV-1 gene therapy due to its strong inhibition of HIV-1 replication in the cells.

Acknowledgments

This work was supported in part by a Grant-in-Aid for High Technology Research, No. 09309011, from the Ministry of Education, Science, Sports and Culture, Japan, and by a grant from the Japan Society for the Promotion of Science in the "Research for the Future" program (JSPS-RFTF97L00593) and Research Grant from the Human Science Foundation (HIV-SA-14719).

References

[1] R.J. Miller, J.S. Cairns, S. Bridges, N. Sarver, Human immunodeficiency virus and AIDS: insights from animal lentiviruses, J. Virol. 74 (2000) 7187–7195.

[2] V. Seroude, G. Audoly, P. Gluschankof, M. Suzan, Tryptophan 95, an amino acid residue of the Caprine arthritis encephalitis virus vif protein, which is essential for virus replication, Virology 280 (2001) 232–242.

[3] P. Metharom, S. Takyar, H.Q. Xia, K.A. Ellem, G.E. Wilcot, M.Q. Wei, Development of disabled, replication-defective gene transfer vectors from the Jembrana disease virus, a new infectious agent of cattle, Vet. Microbiol. 80 (2001) 9–22.

[4] U. Chatterji, C.K. Grant, J.H. Elder, Feline immunodeficiency virus *Vif* localizes to the nucleus, J. Virol. 74 (2000) 2533–2540.

[5] M. Dettenhofer, S. Cen, B.A. Carlson, L. Kleiman, X.F. Yu, Association of human immunodeficiency virus type-1 *Vif* with RNA and its role in reverse transcription, J. Virol. 74 (2000) 8938–8945.

[6] J. Goncalves, P. Jallepalli, D.H. Gabuzda, Subcellular localization of the *Vif* protein of human immunodeficiency virus type 1, J. Virol. 70 (1994) 704–712.

[7] J. Goncalves, F. Silva, A. Freitas-Vieira, M. Santa-Marta, R. Malho, X. Yang, D. Gabuzda, C. Barbas III, Functional neutralization of HIV-1 *Vif* protein by intracellular immunization inhibits reverse transcription and viral replication, J. Biol. Chem. 277 (2002) 32036–32045.

[8] T. Henzler, A. Harmache, H. Herrman, H. Spring, M. Suzan, G. Audoly, T. Panek, V. Bosch, Fully functional, naturally occurring and C-terminally truncated variant human immunodeficiency virus (HIV) *Vif* does not bind to HIV *Gag* but influences intermediate filament structure, J. Gen. Virol. 82 (2001) 561–573.

[9] M.K. Karczewski, K. Strebel, Cytoskeleton association and virion incorporation of the human immunodeficiency virus type 1 *Vif* protein, J. Virol. 70 (1996) 494–507.

[10] J.H. Simon, D.L. Miller, R.A. Fouchier, M.A. Soares, K.W. Peden, M.H. Malim, The regulation of primate immunodeficiency virus infectivity by *Vif* is cell species restricted: a role for *Vif* in determining virus host range and cross-species transmission, EMBO J. 17 (1998) 1259–1267.

[11] D.H. Gabuzda, K. Lawrence, E. Langhoff, E. Terwilliger, T. Dorfman, W. Haseltine, J. Sodroski, Role of *vif* in replication of human immunodeficiency virus type 1 in CD^{4+} T lymphocytes, J. Virol. 66 (1992) 6489–6495.

[12] U. Von Schwedler, J. Song, C. Aiken, D. Trono, *Vif* is crucial for human immunodeficiency virus type 1 proviral DNA synthesis in infected cells, J. Virol. 67 (1993) 4945–4955.

[13] P. Sova, V. Volsky, Efficiency of viral DNA synthesis during infection of permissive and nonpermissive cells with *vif*-negative human immunodeficiency virus type 1, J. Virol. 67 (1993) 6322–6326.

[14] R.A. Fouchier, J.H. Simon, A.B. Jaffe, M.H. Malim, Human immunodeficiency virus type-1 *Vif* does not influence expression or virion incorporation of gag-, pol-, and env-encoded proteins, J. Virol. 70 (1996) 8263–8269.

[15] A.M. Sheehy, N.C. Gaddis, J.D. Choi, M.H. Malim, Isolation of a human gene that inhibits HIV-1 infection and is suppressed by the viral *Vif* protein, Nature 418 (2002) 646–650.

[16] M. Roberto, D. Chen, B. Schrofelbauer, F. Navarro, R. Konig, B. Boliman, C. Munk, H. Nymark-McMahon, N.R. Landau, Species-specific exclusion of APOBEC3G from HIV-1 virions by *Vif*, Cell 114 (2003) 21–31.

[17] N. Madani, R. Millette, E.J. Platt, M. Marin, S.L. Kozak, D.B. Bloch, D. Kabat, Implication of the lymphocyte-specific nuclear body protein Sp140 in an innate response to human immunodeficiency virus type 1, J. Virol. 76 (2002) 11133–11138.

[18] J.H. Simon, N.C. Gaddis, R.A. Fouchier, M.H. Malim, Evidence for a newly discovered cellular anti-HIV-1 phenotype, Nat. Med. 4 (1998) 1397–1400.

[19] J.H. Simon, A.M. Sheehy, E.A. Carpenter, R.A. Fouchier, M.H. Malim, Mutational analysis of the human immunodeficiency virus type 1 *Vif* protein, J. Virol. 73 (1999) 2675–2681.

[20] S.H. Bridges, N. Sarver, Gene therapy and immune restoration for HIV disease, Lancet 345 (1995) 427–475.

[21] J.O. Ojwang, A. Hampel, D.J. Looney, F. Wong-Staal, J. Rappaport, Inhibition of human immunodeficiency virus type 1 expression by hairpin ribozyme, Proc. Natl. Acad. Sci. USA 89 (1992) 10802–10806.

[22] M.J. Potash, G. Bentsman, T. Muir, C. Krachmarov, P. Sova, D.J. Volsky, Peptide inhibitors of HIV-1 protease and viral

infection of peripheral blood lymphocytes based on HIV-1 *Vif*, Proc. Natl. Acad. Sci. USA 95 (1998) 13865–13868.
[23] M.R. Mautino, R.A. Morgan, Inhibition of HIV-1 replication by novel lentiviral vectors expressing transdominant Rev and HIV-1 env antisense, Gene Ther. 7 (2002) 421–431.
[24] M.R. Mautino, R.A. Morgan, Enhanced inhibition of human immunodeficiency virus type 1 replication by novel lentiviral vectors expressing human immunodeficiency virus type 1 envelope antisense RNA, Hum Gene Ther. 9 (2002) 1027–1037.
[25] F. Gennari, M.A. Biasolo, E. Cancellotti, A. Radaelli, C. De Giuli Morghen, I. Bozzoni, P.M. Cereda, C. Mengoli, G. Palu, C. Parolin, Additive and antagonist effects of therapeutic gene combinations for suppression of HIV-1 infection, Antiviral Res. 1 (2002) 5577–5590.
[26] S.F. Ding, R. Lombardi, R. Nazari, S. Joshi, A combination anti-HIV-1 gene therapy approach using a single transcription unit that expresses antisense, decoy, and sense RNAs, and trans-dominant negative mutant Gag and Env proteins, Front Biosci. 7 (2002) 15–28.
[27] D.R. Chadwick, A.M. Lever, Antisense RNA sequences targeting the 5′ leader packaging signal region of human immunodeficiency virus type-1 inhibits viral replication at post-transcriptional stages of the life cycle, Gene Ther. 16 (2000) 1362–1368.
[28] H.K. Chang, R. Gendelman, J. Lisziewicz, R.C. Gallo, B. Ensoli, Block of HIV-1 infection by a combination of antisense tat RNA and TAR decoys: a strategy for control of HIV-1, Gene Ther. 1 (1994) 208–216.
[29] M. Yu, E. Poeschla, F. Wong-Staal, Progress towards gene therapy for HIV infection, Gene Ther. 1 (1994) 13–26.
[30] J. Liu, C. Woffendin, Z.Y. Yang, G.J. Nabel, Regulated expression of a dominant negative form of Rev improves resistance to HIV replication in T cells, Gene Ther. 1 (1994) 32–37.
[31] G. Sczakiel, M. Homann, K. Rittner, Computer-aided search for effective antisense RNA target sequences of the human immunodeficiency virus type 1, Antisense Res. Dev. 3 (1993) 45–52.
[32] M.A. Biasolo, A. Radaelli, L. del Pup, E. Franchin, C. De Giuli-Morghen, G. Palu, A new antisense tRNA construct for the genetic treatment of human immunodeficiency virus type 1 infection, J. Virol. 70 (1996) 2154–2161.
[33] H. Cohli, B. Fan, R.L. Joshi, A. Ramezani, X. Li, S. Joshi, Inhibition of HIV-1 multiplication in a human CD^{4+} lymphocytic cell line expressing antisense and sense RNA molecules containing HIV-1 packaging signal and Rev response element(s), Antisense Res. Dev. 4 (1994) 19–29.
[34] S. Joshi, A. Van Brunschot, S. Asad, I. van der Elst, S.E. Read, A. Bernstein, Inhibition of human immunodeficiency virus type 1 multiplication by antisense and sense RNA expression, J. Virol. 65 (1991) 5524–5530.
[35] M. Shahabuddin, A.S. Khan, Inhibition of human immunodeficiency virus type 1 by packageable, multigenic antisense RNA, Antisense Nucleic Acid Drug Dev. 10 (2000) 141–151.
[36] P.F. Torrence, R.K. Maitra, K. Lesiak, S. Khamnei, A. Zhou, R.H. Silverman, Targeting RNA for degradation with a (2′–5′) oligoadenylate-antisense chimera, Proc. Natl. Acad. Sci. USA 90 (1993) 1300–1304.
[37] W.S. Park, N. Miyano-Kurosaki, M. Hayahune, E. Nakajima, T. Matsuzaki, F. Shimada, H. Takaku, Prevention of HIV-1 infection in human peripheral blood mononuclear cells by specific RNA interference, Nucleic Acids Res. 30 (2002) 4830–4835.
[38] Y. Miura, N. Misawa, N. Meada, Y. Inagaki, Y. Tanaka, M. Ito, N. Koyagaki, N. Yamamoto, H. Yagita, H. Mizusawa, Y. Koyanagi, Contribution of tumor necrosis factor-related apoptosis-inducing ligand (TRAIL) to apoptosis of human CD^{4+} T cells in HIV-1 infected hu-PBL-NOD-SCID mice, J. Exp. Med. 193 (2001) 651–659.
[39] A. Adachi, H.E. Gendelman, S. Koenig, T. Folks, R. Willey, A. Rabson, M.A. Martin, Production of acquired immunodeficiency syndrome-associated retrovirus in human and nonhuman cells transfected with an infectious molecular clone, J. Virol. 59 (1986) 284–291.
[40] A. Sakai, Y. Hirabashi, S. Aizawa, M. Tanaka, S. Ida, S. Oka, Investigation of a new p24 antigen detection system by the chemiluminescence-enzyme-immuno-assay, J. Japn. Assoc. Infect. Dis. 73 (1999) 205–212.
[41] L.J. Reed, H.A. Muench, A simple method of estimating fifty percent endpoints, Am. J. Hyg. 27 (1938) 493–497.
[42] D.F. Purcell, M.A. Martin, Alternative splicing of human immunodeficiency virus type 1 mRNA modulates viral protein expression, replication, and infectivity, J. Virol. 67 (1993) 6365–6378.

Stereoselective Synthesis of [L-Arg-L/D-3-(2-naphthyl)alanine]-Type (*E*)-Alkene Dipeptide Isosteres and Its Application to the Synthesis and Biological Evaluation of Pseudopeptide Analogues of the CXCR4 Antagonist FC131

Hirokazu Tamamura,*,† Kenichi Hiramatsu,† Satoshi Ueda,† Zixuan Wang,‡ Shuichi Kusano,§ Shigemi Terakubo,§ John O. Trent,∥ Stephen C. Peiper,‡ Naoki Yamamoto,⊥ Hideki Nakashima,§ Akira Otaka,† and Nobutaka Fujii*,†

Graduate School of Pharmaceutical Sciences, Kyoto University, Sakyo-ku, Kyoto 606-8501, Japan, Medical College of Georgia, Augusta, Georgia 30912, St. Marianna University, School of Medicine, Miyamae-ku, Kawasaki 216-8511, Japan, James Graham Brown Cancer Center, University of Louisville, Louisville, Kentucky 40202, and Tokyo Medical and Dental University, School of Medicine, Bunkyo-ku, Tokyo 113-8519, Japan

Received July 18, 2004

L,L-Type and L,D-type (*E*)-alkene dipeptide isosteres (EADIs) that have unnatural side chains at the α-position were synthesized by the combination of stereoselective aziridinyl ring-opening reactions and organozinc−copper-mediated *anti*-S_N2' reactions toward a single substrate of γ,δ-*cis*-γ,δ-epimino (*E*)-α,β-enoate. The utility of this methodology was demonstrated by the stereoselective synthesis of a set of diastereomeric EADIs of L-Arg-L/D-3-(2-naphthyl)alanine (Nal) that is contained in a small CXCR4 antagonist FC131 [*cyclo*(-D-Tyr-Arg-Arg-Nal-Gly-)]. Furthermore, a (Nal-Gly)-type EADI was synthesized by samarium diiodide (SmI_2)-induced reduction of a γ-acetoxy-α,β-enoate. Several FC131 analogues, in which these EADIs were inserted for reduction of their peptide character, were synthesized with analogues containing reduced amide-type dipeptide isosteres to investigate the importance of these amide bonds for anti-HIV and CXCR4-antagonistic activity.

Introduction

The practical utility of (*E*)-alkene dipeptide isosteres (EADIs) has been intensively investigated in structure−activity relationship (SAR) studies of biologically active peptides toward development of peptide-lead drugs.[1−7] Backbone replacements of amide bonds in peptides by EADIs provide information on the contributions of the corresponding amide bonds on biological activity. We previously established a completely stereocontrolled synthetic process for L,L-type and L,D-type EADIs starting from L-amino acid.[8,9] As shown in Scheme 1, treatment of *N*-aryl-γ,δ-*cis*-γ,δ-epimino (*E*)-α,β-enoates (*cis*-(*E*)-enoates) **1** with methanesulfonic acid (MSA) gives γ-mesyloxy-α,β-enoates **2**, which can be converted into L,D-type EADIs **3** by organocopper-mediated α-alkylation via *anti*-S_N2' reactions, whereas organocopper treatment of *cis*-(*E*)-enoates **1** affords L,L-type EADIs **4**. However, this synthetic procedure has not yet been optimized, because it involves a potential limitation on the introduction of functional groups into the side chain (R^3) at the α-position. In a standard procedure, organocopper reagents, which were prepared by CuCN and RLi or RMgX (X = Cl or Br), are used for α-alkylation.[2,4] In the α-alkylation of the synthesis of (Xaa-L/D-Glu)-type EADIs,[10] organozinc−copper reagents are used, which are prepared from $IZnCH_2CH_2CO_2R$ and CuCN.[11−15] In this study, to demonstrate the general utility of organozinc−copper reagents, a set of EADIs of L-Arg-L/D-3-(2-naphthyl)alanine (Nal) were synthesized as model compounds via the γ,δ-*cis*-γ,δ-epimino (*E*)-α,β-enoate by the combination of MSA-mediated aziridinyl ring-opening reactions and α-alkylation with organozinc−copper reagents, which were prepared from 2-naphthylmethylZnBr and CuCN. The dipeptide sequence, Arg-Nal, is part of the low molecular weight CXCR4 antagonist, FC131, which was recently developed by us (Figure 1).[16]

Scheme 1[a]

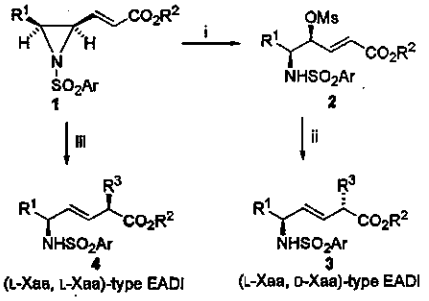

[a] R^1, R^2, R^3 = alkyl; Ar = 2,4,6-trimethylphenylsulfonyl (Mts) or Ts. Reagents: (i) MsOH; (ii) $R^3Cu(CN)MgX\cdot BF_3$ (X = Cl or Br) or $R^3Cu(CN)Li\cdot BF_3$; (iii) $R^3Cu(CN)MgX\cdot 2LiX$ (X = Cl or Br) or $R^3Cu(CN)Li\cdot 2LiX$.

In this study, to demonstrate the general utility of organozinc−copper reagents, a set of EADIs of L-Arg-L/D-3-(2-naphthyl)alanine (Nal) were synthesized as model compounds via the γ,δ-*cis*-γ,δ-epimino (*E*)-α,β-enoate by the combination of MSA-mediated aziridinyl ring-opening reactions and α-alkylation with organozinc−copper reagents, which were prepared from 2-naphthylmethylZnBr and CuCN. The dipeptide sequence, Arg-Nal, is part of the low molecular weight CXCR4 antagonist, FC131, which was recently developed by us (Figure 1).[16]

CXCR4 is a chemokine receptor, which is involved in cell progression and metastasis of several types of cancer,[17−19] HIV entry,[20] and rheumatoid arthritis.[21,22] Thus, several inhibitors directed against CXCR4 have been developed.[23−27] We previously found a highly potent CXCR4 antagonist, T140, which is a 14-mer

* Corresponding authors. Tel: +81 75 753 4551, Fax: +81 75 753 4570, E-mail: tamamura@pharm.kyoto-u.ac.jp; nfujii@pharm.kyoto-u.ac.jp.
† Kyoto University.
‡ Medical College of Georgia.
§ St. Marianna University.
∥ University of Louisville.
⊥ Tokyo Medical and Dental University.

10.1021/jm049429h CCC: $30.25 © 2005 American Chemical Society
Published on Web 12/21/2004

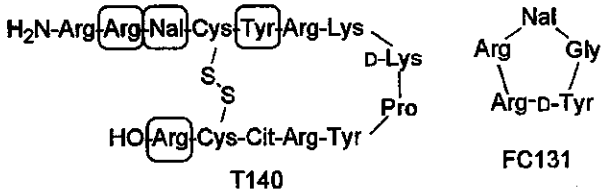

Figure 1. Structures of T140 and its downsized peptide FC131. Circled residues are the indispensable residues of T140 for the expression of strong CXCR4-antagonistic activity. Nal = L-3-(2-naphthyl)alanine, Cit = L-citrulline.

peptide with a disulfide bridge, and we identified four critical residues: Arg^2, Nal^3, Tyr^5, and Arg^{14} (Figure 1).[28-30] Molecular-size reduction of T140 based on the structural requirement led to the discovery of FC131, which has a cyclic pentapeptide template,[31-37] with CXCR4-antagonistic and anti-HIV activity comparable to those of T140.[16] We wish to investigate contributions of each amide bond in FC131 to the biological activity in order to develop pseudopeptides, in which the peptide character is reduced to obtain more druglike structures. For this purpose, EADIs and reduced amide-type dipeptide isosteres (RADIs) of Arg-Nal and Nal-Gly are required, because the amide bonds between Arg^2 and Nal^3 and between Nal^3 and Cys^4 were found to be cleaved by treatment of T140 analogues with rat liver homogenates.[38,39] Thus, (L-Arg-L/D-Nal)-type EADIs were synthesized in the study described here, and a (Nal-Gly)-type EADI was also synthesized by another method using the samarium diiodide (SmI_2)-induced reduction of a γ-acetoxy-α,β-enoate.[40,41] RADIs of Arg-Nal and Nal-Gly were prepared by a standard method of reductive amination. Then, several FC131 analogues, in which the above isosteres were introduced, were synthesized to identify the biological importance of these amide bonds.

Results and Discussion

Synthesis of (L-Arg-L/D-Nal)-Type EADIs. (L-Arg-L/D-Nal)-type EADIs were synthesized via the same key intermediate *N*-2-nitrobenzenesulfonyl (Ns)-γ,δ-*cis*-γ,δ-epimino (*E*)-α,β-enoate, **9**, as synthetic model compounds for the investigation of the feasibility of α-alkylation using organozinc−copper reagents as well as precursor dipeptide isosteres used for the synthesis of partial nonpeptide analogues of FC131 (Scheme 2). Boc-Arg(Mts)-OMe (Mts = 2,4,6-trimethylbenzenesulfonyl) **5** was treated successively with diisobutylaluminum hydride (DIBAL-H) and vinylmagnesium chloride (CH_2=CHMgCl) to give exclusively the *threo*-amino alcohol **6** (a separable mixture of allyl alcohol **6**/*erythro*-isomer of **6** = 12:1). N^{α}-Ns protection[42,43] after the cleavage of the N^{α}-Boc group of **6** with HCl/dioxane followed by successive treatments consisting of the Mitsunobu reaction,[44] ozonolysis, and the modified Horner−Wadsworth−Emmons olefination[45] afforded *cis*-(*E*)-enoate **9**. *Anti*-S_N2' reaction of **9** with an organozinc−copper reagent,[11-15] 2-naphthylmethylCu(CN)-ZnBr·2LiCl, afforded an L,L-type EADI **10**, in which a (2*R*)-2-naphthylmethyl side chain was incorporated at the α-position, stereoselectively in 83% yield (diastereoselection > 99:1 from NMR analysis). N^{α}-Fmoc substitution for the N^{α}-Ns group of **10** followed by selective deprotection of the benzyl ester using thioanisole/TFA afforded a desired EADI, Fmoc-L-Arg(Mts)-ψ[(*E*)-CH=CH]-L-Nal-OH, **12**. Alternatively, exposure of **9** to MSA/$CHCl_3$ afforded exclusively δ-aminated γ-mesyloxy-α,β-enoate **13** by regio- and stereoselective S_N2 ring-opening reaction at the γ-carbon of **9**. Mesylate **13** was successively treated by an organozinc−copper reagent, 2-naphthylmethylCu(CN)ZnBr·BF_3, to afford an L,D-type EADI **14**, in which a (2*S*)-2-naphthylmethyl side chain was incorporated at the α-position, stereoselectively via an *anti*-S_N2'mechanism in 67% yield (diastereoselection > 99:1 from NMR analysis). **14** was similarly converted into another desired EADI, Fmoc-L-Arg(Mts)-ψ[(*E*)-CH=CH]-D-Nal-OH, **16**. As such, α-alkylation of both a *cis*-(*E*)-enoate and its ring-opened product using organozinc−copper reagents was successfully performed in the synthesis of (L-Arg-L/D-Nal)-type EADIs. An *N*-Ns group could be used in this synthetic scheme as an orthogonal *N*-protecting (activating) group instead of an *N*-Mts or *N*-Ts group. Relative configurations of the allyl alcohols (**6** and its erythro isomer) were determined by comparative nuclear Overhauser effect (NOE) measurements of these oxazolidinone derivatives **17** and **18** (Scheme 2).[2] The (*E*)-geometry of the double bond in the synthesized EADIs was assigned based on the coupling constant of the two olefinic protons on ^1H NMR analysis.

Synthesis of (L-Nal-Gly)-Type EADI. An (L-Nal-Gly)-type EADI was synthesized as shown in Scheme 3. Boc-L-Nal-OMe **19** was treated sequentially with DIBAL-H and CH_2=CHMgCl to give a diastereomixture of allyl alcohol **20**. Acetylation of **20** followed by ozonolysis and the modified Horner−Wadsworth−Emmons olefination afforded a γ-acetoxy-α,β-unsaturated ester **22**. Acetate **22** was reduced with SmI_2−^{t}BuOH to yield an (L-Nal-Gly)-type EADI **23** in 95% yield,[40,41] followed by deprotection of the N^{α}-Boc group and *tert*-butyl ester with TFA and reprotection with an N^{α}-Fmoc group to afford the desired EADI, Fmoc-L-Nal-ψ[(*E*)-CH=CH]-Gly-OH, **24**.

Synthesis of RADIs of Arg-Nal and Nal-Gly. (L-Arg-L-Nal)- and (L-Nal-Gly)-type RADIs were prepared for comparative studies. As shown in Scheme 4, Arg- and Nal-derived Weinreb amides **25** and **29** were treated with DIBAL-H to afford the corresponding aldehyde derivatives. Subsequently, reductive amination of the aldehydes was performed by treatments with carboxy-protected amino acids in the presence of acetic acid and sodium triacetoxy borohydride [$NaBH(OAc)_3$] to afford secondary amines **26** and **30**, respectively.[46] Protection of the *sec*-amino groups with Cbz groups followed by deprotection of the N^{α}-Boc group and *tert*-butyl ester with TFA and reprotection with an N^{α}-Fmoc group afforded the desired RADIs, Fmoc-L-Arg(Mts)-ψ-[CH_2−N(Cbz)]-L-Nal-OH, **28**, and Fmoc-L-Nal-ψ[CH_2−N(Cbz)]-Gly-OH, **32**, respectively.

Synthesis of Cyclic Pseudopeptides. The protected peptide chains were constructed on a hydrazino resin **34** by Fmoc-based solid-phase synthesis using ^{t}Bu and 2,2,4,6,7-pentamethyldihydrobenzofuran-5-sulfonyl (Pbf) groups for side-chain protection of D-Tyr and Arg, respectively (Scheme 5). N^{α}-Fmoc-protected dipeptide isosteres, EADIs **12**, **16**, and **24** and RADIs **28** and **32**, were similarly condensed. In the synthesis of cyclic pseudopeptides, two steps of deprotection/cleavage were adopted to prevent guanidino groups of Arg from

Scheme 2[a]

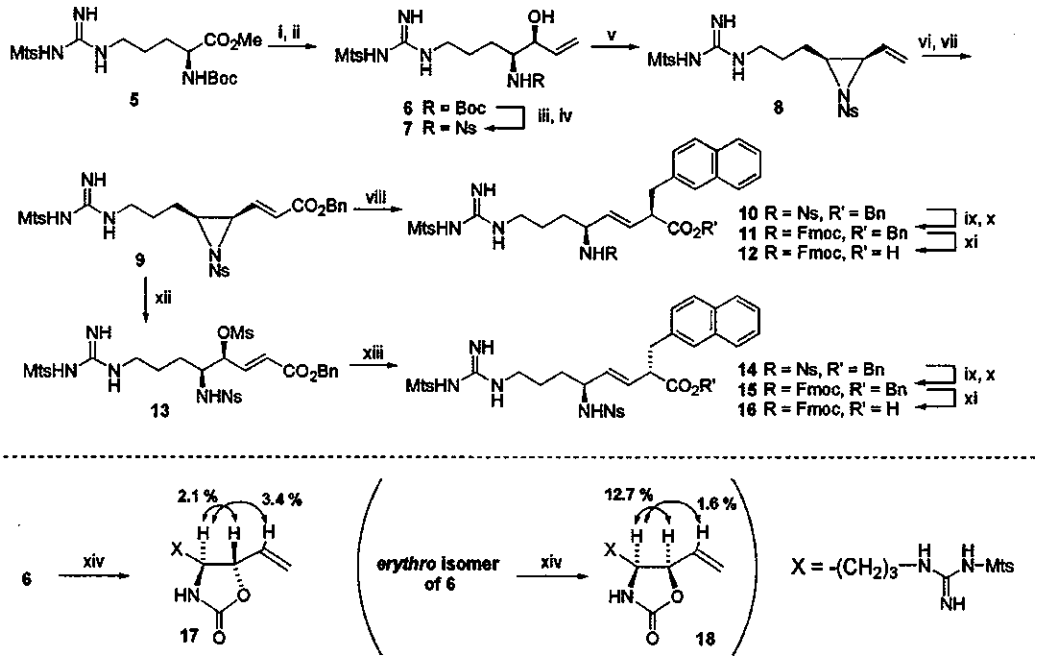

[a] Reagents: (i) DIBAL-H; (ii) CH_2=CHMgCl; (iii) HCl, anisole; (iv) Ns-Cl, pyridine; (v) Ph_3P, DEAD; (vi) O_3, then Me_2S; (vii) $(EtO)_2P(O)CH_2CO_2Bn$, LiCl, DIPEA; (viii) 2-naphthylmethylCu(CN)ZnBr·2LiCl; (ix) PhSH, K_2CO_3; (x) Fmoc-OSu, Et_3N; (xi) thioanisole, TFA; (xii) MsOH; (xiii) 2-naphthylmethylCu(CN)ZnBr·BF_3; (xiv) NaH.

Scheme 3[a]

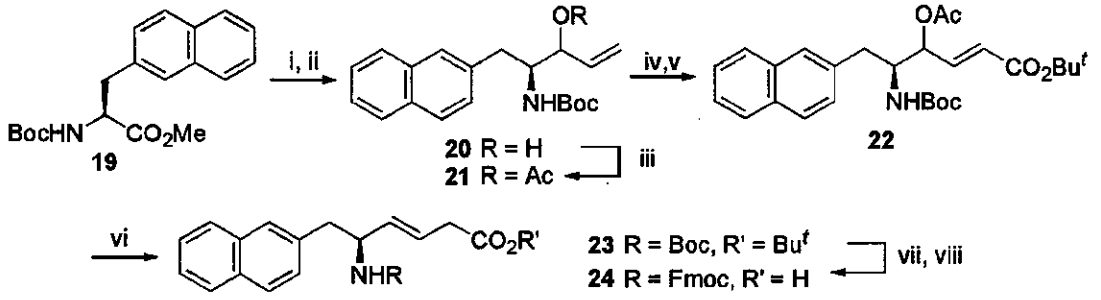

[a] Reagents: (i) DIBAL-H; (ii) CH_2=CHMgCl; (iii) Ac_2O, DMAP, pyridine; (iv) O_3, then Me_2S; (v) $(EtO)_2P(O)CH_2CO_2{}^tBu$, LiCl, DIPEA; (vi) SmI_2, ^tBuOH; (vii) anisole, TFA; (viii) Fmoc-OSu, Et_3N.

Scheme 4[a]

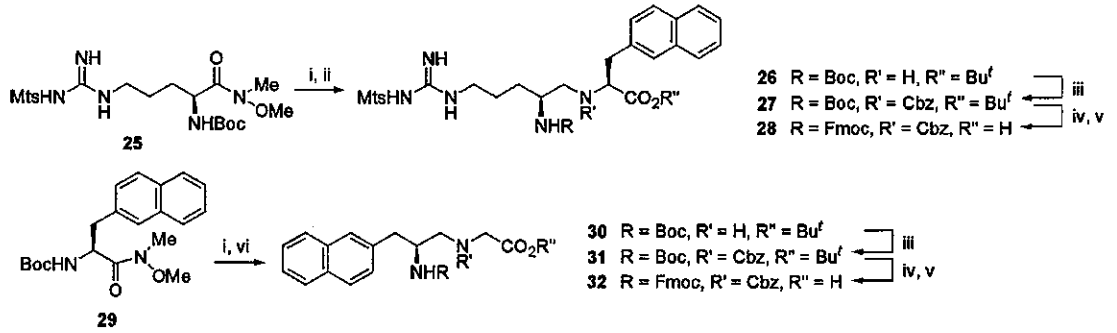

[a] Reagents: (i) DIBAL-H; (ii) H-Nal-O^{t}Bu, AcOH, $NaBH(OAc)_3$; (iii) Cbz-Cl, Et_3N; (iv) anisole, TFA; (v) Fmoc-OSu, Et_3N; (vi) H-Gly-O^{t}Bu, AcOH, $NaBH(OAc)_3$.

participating in cyclizing reaction as follows. After construction of peptide chains, pseudopeptide hydrazides **36** were obtained by cleavage from the resin **35** using 10% TFA/$CHCl_3$ without cleavage of Pbf, Mts, and Cbz groups (first deprotection). Cyclization of linear pseudopeptides by the azide procedure[47] in highly

Scheme 5[a]

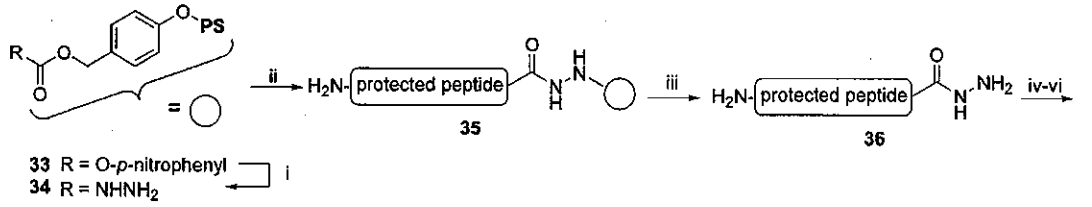

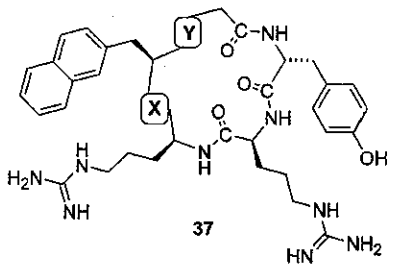

Compd.	Sequence (*cyclo*)	X	Y
FC131	(-D-Tyr-Arg-Arg-Nal-Gly-)	-CO-NH-	-CO-NH-
37a	(-D-Tyr-Arg-Arg-Nal-Gly-)	-CH=CH-	-CO-NH-
37b	(-D-Tyr-Arg-Arg-Nal-Gly-)	$-CH_2$-NH-	-CO-NH-
37c	(-D-Tyr-Arg-Arg-Nal-Gly-)	-CO-NH-	-CH=CH-
37d	(-D-Tyr-Arg-Arg-Nal-Gly-)	-CO-NH-	$-CH_2$-NH-
37e	(-D-Tyr-Arg-Arg-D-Nal-Gly-)	-CO-NH-	-CO-NH-
37f	(-D-Tyr-Arg-Arg-D-Nal-Gly-)	-CH=CH-	-CO-NH-

[a] Reagents: (i) $NH_2NH_2 \cdot H_2O$; (ii) Fmoc-based SPPS; (iii) TFA; (iv) HCl, isoamyl nitrite; (v) DIPEA; (vi) 1 M TMSBr–thioanisole/TFA, *m*-cresol, 1,2-ethanedithiol.

Table 1. Activity and Cytotoxicity of the Synthetic Compounds

compound (no.)	CC_{50}[a] (μM)	EC_{50}[b] (μM)	IC_{50}[c] (μM)
FC131	> 100	0.073	0.0045 ± 0.0018
37a	> 100	2.4	31–100[d]
37b	> 100	> 100	> 100
37c	> 100	2.4	0.18 ± 0.10
37d	> 100	0.98	0.032 ± 0.011
37e	> 100	1.9	0.19 ± 0.071
37f	> 100	9.1	21
T140	> 10	0.035	0.0039 ± 0.0004
AZT	57	0.018	

[a] CC_{50} values are based on the reduction of the viability of mock-infected MT-4 cells. Because the cytotoxicity of T140 was previously evaluated as CC_{50} > 40 μM, further estimation at high concentrations was omitted in this study. [b] EC_{50} values are based on the inhibition of HIV-induced cytopathogenicity in MT-4 cells. [c] IC_{50} values are based on the inhibition of [^{125}I]-SDF-1-binding to CXCR4 transfectants of CHO cells. All data are the mean values for at least three independent experiments. [d] **37a** showed significant antagonistic activity in 100 μM but hardly showed activity in 31 μM.

diluted dimethylformamide (DMF) solution followed by deprotection of Pbf, Mts, and Cbz groups with 1 M TMSBr–thioanisole/TFA (second deprotection) gave the desired cyclic pseudopeptides **37**.

Biological and Conformational Evaluation of Synthetic Cyclic Pseudopeptides. Anti-HIV activity based on the inhibition of HIV-1-induced cytopathogenicity in MT-4 cells was evaluated using the 3-(4,5-dimethylthiazol-2-yl)-2,5-diphenyltetrazolium bromide (MTT) method.[48] CXCR4-antagonistic activity was evaluated by the inhibition of [^{125}I]-SDF-1-binding to CXCR4 transfectants of CHO cells.[49] **37a**, an (L-Arg-L-Nal)-type EADI containing FC131 analogue, showed moderate anti-HIV activity (EC_{50} = 2.4 μM) and CXCR4-antagonistic activity (100 μM > IC_{50} > 31 μM). Introduction of an EADI into the Arg-Nal sequence caused a remarkable decrease in anti-HIV activity (33-fold lower activity). NMR and simulated annealing molecular dynamics (SA-MD) analysis of **37a** showed a pseudopeptide backbone structure with a nearly symmetrical pentagonal shape similar to that of FC131,[16] excluding the difference between the orientation of two protons in the (*E*)-alkene unit of **37a** and that of the carbonyl oxygen/amino proton in the Arg-Nal amide bond of FC131 (Figure 2a).[50] Substitution for the amide bond with the EADI caused an inversion of the olefinic plane (180° rotation of pseudo ψ and ϕ bonds), possibly due to dissolution of the 1,3-pseudo-allylic strain between the carbonyl group of Arg and the side chain of Nal. Introduction of an EADI into the Arg-D-Nal sequence of **37e** (an FC131 epimer, EC_{50} = 1.9 μM, IC_{50} = 190 nM) also caused a significant but moderate decrease in anti-HIV activity (the activity of **37f** is 5-fold lower than that of **37e**). The amide bonds of the Arg-L/D-Nal sequences were necessary for high potency. These results suggested that either a deletion of the hydrogen bond interaction with CXCR4 by the insertion of an EADI or an increase in hydrophobicity might be unsuitable. **37b**, an (L-Arg-L-Nal)-type RADI-containing FC131 analogue, did not show anti-HIV or CXCR4-antagonistic activity up to the concentration of 100 μM, suggesting that the planar nature of the amide bond is critical to maintain the pentagonal global conformation for high anti-HIV activity and that the replacement of the amide bond with RADI causes a conformational change of FC131. **37c**, an (L-Nal-Gly)-type EADI-containing FC131 analogue, showed almost the same anti-HIV activity (EC_{50} = 2.4 μM) as **37a** containing an (L-Arg-L-Nal)-type EADI. NMR and SA-MD analysis of **37c** showed a similar backbone structure with FC131 (Figure 2b).[50] The Nal-Gly amide bond was replaced by the EADI without an inversion of the olefinic plane. **37d**, an (L-Nal-Gly)-type RADI-containing FC131 analogue, exhibited relatively higher anti-HIV and CXCR4-antagonistic activities (EC_{50} = 0.98 μM, IC_{50} = 32 nM) than **37c** (IC_{50} = 180 nM), although these activities were weaker than those of FC131. These results also indicated an importance of the amide bond of the Nal-Gly sequence, as in the case of the Arg-Nal amide bond.